CONFIDENCE OF SUCCESS IN MULTI-CRITERIA OPTIMIZATION OF MULTI-DISCIPLINARY SHIP DESIGN MODELS

Emanuel Klasén

SUBMITTED TO

THE DEPARTMENT OF AEROSPACE AND OCEAN ENGINEERING,
VIRGINIA POLYTECHNIC INSTITUTE AND STATE UNIVERSITY, BLACKSBURG, VA, USA

SUPERVISOR: Dr. Wayne Neu, AOE VT

AND

THE DIVISION OF NAVAL SYSTEMS (MSY),
DEPARTMENT OF AERONAUTICAL AND VEHICLE ENGINEERING,
ROYAL INSTITUTE OF TECHNOLOGY (KTH), STOCKHOLM, SWEDEN
IN ACCORDANCE WITH THE REQUIREMENTS OF THE COURSE
4B1014 MASTER OF SCIENCE THESIS IN NAVAL ARCHITECTURE
FOR THE PARTIAL FULFILLMENT OF A DEGREE OF
MASTER OF SCIENCE IN NAVAL ARCHITECTURE

EXAMINER: Ph.D. Jakob Kuttenkeuler, MSY AVE KTH

CONFIDENCE OF SUCCESS IN MULTI-CRITERIA OPTIMIZATION OF MULTI-DISCIPLINARY SHIP DESIGN MODELS

Emanuel Klasén, March 2005

Dept. of Aerospace and Ocean Engineering
Virginia Polytechnic Institute and State University
215 Randolph Hall
Blacksburg VA, 24061, USA
+1-540-231-6611

Div. of Naval Systems (MSY)
Dept. of Aerospace and Vehicle Engineering
Royal Institute of Technology (KTH)
100 44 Stockholm, Sweden
+46-8-7909130

CONFIDENCE OF SUCCESS IN MULTI-CRITERIA OPTIMIZATION
OF MULTI-DISCIPLINARY SHIP DESIGN MODELS

Emanuel Klasén

ABSTRACT

Decision makers are increasingly demanding decision instruments which account for uncertainties in the design process. This demand is partly raised due to the escalating usage of multi-disciplinary models and multi-criteria optimization in many design areas. Design optimization has commonly been formulated as a deterministic process. Since optimization algorithms tend to push a solution to one or more constraint boundaries, even slight uncertainties in the problem formulation may cause a deterministic solution to degenerate. Hence, without handling uncertainty in the optimization process, truly good design solutions will not be found.

The traditional way to handle uncertainties has been based upon the use of crude safety factors. Another way is to handle uncertainties with a probabilistic approach, producing a measure of the confidence of success of a given design, i.e. the probability that the design actually will meet requirements and perform as predicted. By including confidence of success in the optimization process, decision makers will have a better chance of finding robust and reliable designs or further evolvable concepts.

Confidence of success merges robustness and reliability into an unbiased objective in the optimization process. In this paper, the first steps of the Mean Value Method are utilized to approximate constraint and performance attribute responses and calculate probabilities based on the joint distribution of the uncertain variables. Implementation and utilization of confidence of success is demonstrated in a multi-criteria optimization of a simplified ship synthesis model.

The Mean Value Method does not prove to be adequate in the search for optimal solutions in a complex objective space, which can be expected for a multi-disciplinary ship model. However, the method is efficient in well-behaving systems with few uncertainties and could be used as guidance in preliminary or conceptual design situations that require a heavy computational effort.

Keywords: confidence of success, uncertainty, probability, Mean Value Method, multi-criteria optimization, pareto optimal, multi-disciplinary, ship design

TABLE OF CONTENTS

SI units and abbreviations are used throughout the paper unless otherwise stated.

NOMENCLATURE

CDF	Cumulative Distribution Function
CoS	Confidence of Success
CTOC	Total Ownership Cost
DDG51	Reference DP; Arleigh Burke, guided missile destroyer
DP	Design Point
GA	Genetic Algorithm
JCDF	Joint CDF, multi-variable CDF
JPDF	Joint PDF, multi-variable PDF
LSF	Limit State Function
MCS	Monte Carlo Simulation
MCO	Multi-Criteria Optimization
MV	Mean Value Method
OMOE	Overall Measurement of Effectiveness
PDF	Probability Density Function
R_T	Bare hull resistance
RV	Random Variable
W_T	Total ship weight
g	LSF
Z_{ls}	Limit State (value)
μ	Mean or expected value E(X) of a random variable X
σ	Standard deviation of a random variable
δ	Coefficient of variance, $\delta = \sigma / \mu$
ρ	Correlation coefficient

DEFINITIONS

Attribute	Denotes or quantifies system characteristics including design parameters, performance variables, and constraint fulfillment, e.g. length, cost, resistance, or excess power.
Criterion	Measure that is basis for an evaluation; attributes become criteria if decision is based on their outcome.[2] Attributes used in the optimization process and/or for calculating Confidence of Success are referred to as criteria.
Design Point	Specific design variable vector or chromosome.
Objective	A computed characteristic of a solution which we wish to minimize or maximize, e.g. cost, effectiveness, or confidence of success.

Pareto optimum   Non-dominated solution to an optimization problem. A solution is Pareto optimal if it satisfies all constraints and is such that no objective can be improved without causing other objectives to decline.[4] A multi-criteria optimization with conflicting objectives typically result in a number of non-dominated solutions, referred to as a Pareto front or optimal set.

1   Introduction

In recent decades, the usage of multi-disciplinary models and multi-criteria optimization (MCO) has found its way into many design areas. By employing a multi-disciplinary optimization process, the designer can break out of the traditional design-spiral approach. All design variables are allowed to be varied based on their effect on the measure of merit and, hopefully, converge to an optimum design as the process progresses.

Design optimization has commonly been formulated as a deterministic process, based on one design objective with an associated set of design parameters. Since optimization algorithms tend to push a solution to one or more constraint boundaries, the emerged "best" solution might degenerate due to even slight uncertainties in the problem formulation or changes in the operational environment.[1] Sources of uncertainty vary widely, ranging from simulation and modeling errors to economic forecasts, material properties, loading conditions, and the lack of information. Hence, without including uncertainty in the design optimization process, a "best" design can hardly be seen as a good solution.

1.1 Motivation

Decision makers are increasingly demanding a decision making tool which accounts for uncertainties in the design process and produces a measure of the level of confidence of success (CoS) of a given design. Design decisions need to be made with an understanding of the risks introduced by uncertainties in modeling assumptions, inputs, and analyses. The usual way to handle uncertainties has been based upon the use of crude safety factors. Another way is to handle uncertainties with a probabilistic approach.[1]

It is suggested that a probabilistic approach to uncertainties could facilitate an excellent path to true MCO and/or decision-making. However, just as the optimization process itself becomes more complicated with the introduction of MCO, the handling of uncertainties also becomes more intricate. It is insufficient to look at each criterion and its distribution independently, since all attribute values are generated by the same design process and are thus interdependent. The assumption of independent criteria is therefore typically unfounded.[2] Attributes used in the optimization process and/or for calculating CoS are referred to as criteria. These criteria include all objectives and model constraints.

The main approaches in the handling of the probabilistic optimization problem are robust and reliability based design; the difference is the focus of the analysis.

Reliability based design focuses on satisfying, after conversion from a deterministic problem, the probabilistic constraints.

Robust design focuses on performance objectives, which are expanded from deterministic minimimum or maximum objectives to include both mean performance and performance variation. The goals are to drive mean performance towards a target and to minimize performance variance.[1] Though useful in various design systems, implementation of robust design is rare. The reason for this may originate from the complexity and computational burden associated with evaluation of performance variations caused by the uncertainty of a system.[3]

1.2 <u>Objective</u>

The aim of this work is to explore the applicability and usability of the Mean Value Method (MV) to system uncertainties in MCO of multi-disciplinary ship design models. Implementation is carried out on a simplified ship synthesis model, developed at the Department of Aerospace and Ocean Engineering (AOE), Virginia Polytechnic Institute and State University (VT).

This paper merges the robust and reliability approaches into a calculation resulting in a measure of CoS, i.e. the probability that a specific design actually will meet any number of criteria concurrently. The ambition of the approach is to be fast and accurate enough to be used in MCO of systems with heavy computational demands, yielding CoS for every feasible design point (DP). Calculation of probability is made using the first steps of MV, utilizing a simple Taylor series expansion to derive a limit state function (LSF) from criteria responses. The method handles correlation between probabilistic criteria by concurrent application of all LSFs to the joint probability density function (JPDF) of all uncertain system variables.

2   Multi-Criteria Optimization considering uncertainty

In MCO, there is generally no single optimum, because objectives are often conflicting. Instead, the optimization process results in a set of feasible non-dominated solutions or a Pareto optimal set, also referred to as a Pareto front. A solution is Pareto optimal if it satisfies the constraints and is such that no objective can be further improved without causing at least one of the other objectives to deteriorate.[4] Figure 1 is an example of a Pareto front in a two-dimensional objective space, assuming the objective is to minimize the cost and maximize the effectiveness in a deterministic optimization process. Every solution in the objective space is represented by one or possibly more points in the design space. The Pareto front is marked by the bold line at the boundary between the feasible and infeasible regions in the objective space.

If one specific design is to be chosen, the decision should fall on one of the designs making up the Pareto front. What design to choose is up to the decision maker and depends on preferences and the shape of the frontier. One interesting solution region in this case is obviously around the knee of the Pareto front, encircled in Figure 1. These designs yield a high effectiveness per cost ratio and should be considered and probably chosen as the design solution in a deterministic optimization effort, if affordable.

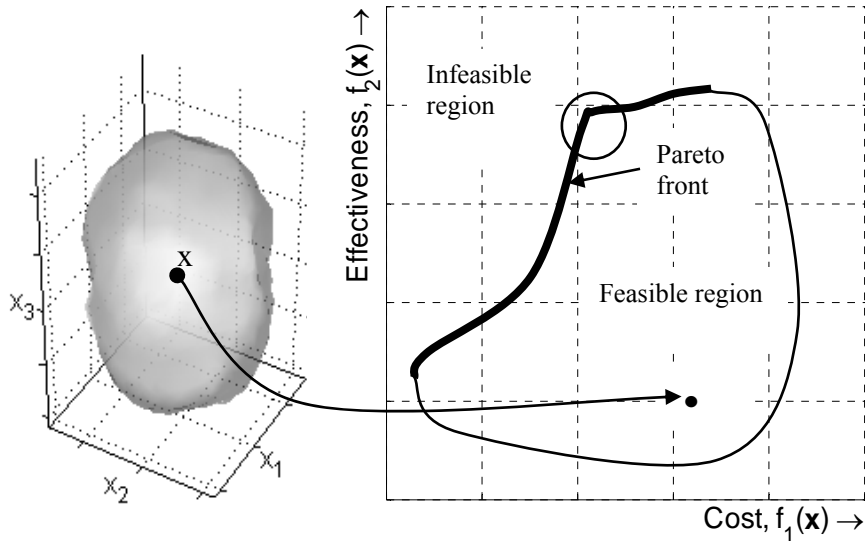
Figure 1   *A design point in the design space, left, corresponds to a solution in the objective space, right. The Pareto front is emphasized by the bold curve coinciding with part of the boundary between the infeasible and feasible regions.*

The deterministic optimization has provided a design solution, accepted by the decision maker, which yields a specific cost and effectiveness. What has not been considered is the probability that the design actually will perform as predicted regarding cost and effectiveness. Due to uncertainties in the model, there might be a great risk that the effectiveness is going to be less and the cost higher than expected, or that this deterministically feasible design actually will have a slim chance of meeting the constraint requirements at all.

Suppose that the probability for a design at the knee to meet all requirements is only 10%. Then the decision maker would most certainly look for a more reliable design among the Pareto optimal designs. The problem is however, that the Pareto front may not include any design with a higher level of CoS since this has been neither part of the optimization objectives nor part of the constraints. The non-dominated solutions with, let's say, at least 60% CoS may not be situated at the boundary between the deterministic feasible and infeasible regions; they may lay well within the feasible region. Hence, either the optimization has to be done with a constraint on CoS, or CoS has to be handled as an objective. By including CoS among the objectives, the decision makers possess the ability to find well performing designs for this objective too. With three objectives, the Pareto front would be a surface in three-dimensional space. This is illustrated in Figure 2 for the three objectives: cost, effectiveness, and CoS.

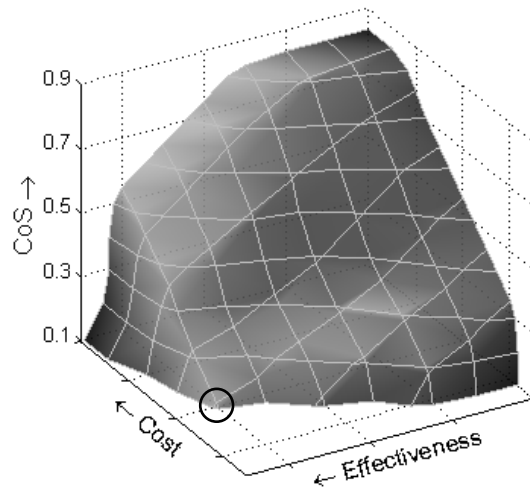*Figure 2*   *An arbitrary Pareto front in 3D space with the objectives to minimize cost and maximize effectiveness and CoS. Encircled is the same knee as in Figure 1, yielding 10% CoS. In this situation, increasing cost or reducing effectiveness raises CoS. There is no solution with a CoS higher than 85%. If this is not satisfactory, the optimization conditions or model needs to be revised.*

2.1 <u>System Uncertainty</u>

System uncertainties come from quantitative or qualitative sources.

Qualitative uncertainties arise from intellectual abstractions of reality. They may come from definition of certain parameters such as quality, deterioration, environmental impact of projects, skill and experience of workers and engineers, and other human factors.

Quantitative sources originate from randomness in physical observation, statistical uncertainty, and modeling uncertainty.

Observation randomness arises due to the fact that repeated measurements of the same physical quantity do not yield the same value, depending on the observer, test procedure, instruments, environmental fluctuations, etc. By collecting a large number of observations, good information about the variability of the measured quantity can be obtained. However, the number of observations that can be collected might be limited, leading to statistical uncertainty.[5]

Model uncertainty represents uncertainties due to the accuracy of analyses performed in the model, i.e. the difference between the computational prediction and the actual performance. Furthermore, in a multi-disciplinary design situation such as a ship model, the prediction of one discipline may be the input of another discipline and vice versa. This causes the uncertainty of each discipline to surge throughout the model due to the interlinking analyses, making it hard to characterize the system output.

2.2 <u>Handling Uncertainty</u>

There are a vast number of suggested computational approaches to handle uncertainty; a few are briefly mentioned here.

Roughly, the different approaches can be divided into three categories: random sampling, Design of Experiments (DOE), and sensitivity based approaches.[1,5] Which category or specific approach provides the most efficient method is strongly dependent on the problem at hand. Typically there is a trade-off between the computational cost and the accuracy. For a MCO of a complex system, e.g. a multi-disciplinary ship model, the algorithm of choice cannot be allowed to evaluate the system too many times, since this would increase the computational time considerably.

The CoS calculation in this work is based on the first steps of MV, which starts with a first order Taylor series expansion, classifying it as a sensitivity based approach. MV is discussed in detail in 2.2.4 Mean Value Methods.

2.2.1 Random Sampling

The most recognizable and basic random sampling technique is Monte Carlo Simulation (MCS) or simple random sampling. MCS is implemented by randomly simulating a design or process, given the stochastic properties of one or more random variables, with focus on characterizing the statistical nature of the responses of interest.[6] This simulation method has long been considered to be the most exact method for calculation of probability distributions of responses from systems dealing with uncertainty. However, MCS typically calls for several thousands of system evaluations; thus for a time consuming analysis, MCS becomes impractical. A remedy for this incongruity could be found in various variance reduction techniques or "Monte Carlo swindles", e.g. Descriptive Sampling[7], Antithetic Variate technique[8] and many more[9].

Descriptive Sampling is an evolution of Latin Hypercube Sampling. These techniques sample from subsets of equal probability of the distributed inputs. Each individual subset is sampled only once, thus reducing the number of necessary system evaluations significantly.

The Antithetic Variate technique produces variance reduction by inducing negative correlation. The number of system calculation cycles can be reduced considerably compared to MCS, if one is not too concerned about complete characteristics of the response. The usability of this technique has been studied in previous work at AOE VT.

2.2.2 Design of Experiments (DOE)

In DOE a design matrix is constructed in a systematic fashion that specifies the values for the uncertain design parameters for each sampled point. Potential values for uncertain design parameters are not defined through probability distributions, but rather are defined by a range, a nominal baseline plus/minus some percent, or through specified values or levels. In this case, each run in the designed experiment is a combination of the defined levels of each parameter. The computational cost is generally less than MCS, however estimates may not be as accurate.[1]

2.2.3 Sensitivity Based Approach

This approach is based on Taylor series expansion, generally either first or second order neglecting higher order terms. Rather than sampling across known distributions or ranges of uncertain design parameters, gradients of performance parameters are calculated with respect to the uncertain design parameters.

A first order Taylor series expansion for a performance response, Y, neglecting higher order terms is:

$$Y(\mathbf{X}) \approx Y(\boldsymbol{\mu}) + \sum_{i=1}^{n} \left(\frac{\partial Y}{\partial X_i} \right)_{\mu} \cdot (X_i - \mu_i)$$

where μ_i is the mean of parameter i and n is the number of uncertain parameters. By setting the uncertain design parameters, $\mathbf{X}$, to their mean value, $\boldsymbol{\mu}$, the response mean performance is calculated as:

$$\mu_y = Y(\boldsymbol{\mu}) \qquad\qquad (1)$$

and the variance, σ_y^2, is given by:

$$\sigma_y^2 = \sum_{i=1}^{n} \left(\frac{\partial Y}{\partial X_i} \right)_{\mu}^2 \cdot \sigma_{xi}^2 \qquad\qquad (2)$$

where σ_{xi} is the standard deviation of parameter i. A first order expansion estimate requires n + 1 analyses for evaluation. It is usually more efficient than MCS, and often more efficient than DOE. However, accuracy is lost when responses are not close to linear.[1]

By increasing the order of the expansion, nonlinear responses can be estimated more accurately, but the computational burden increases significantly. A second order expansion requires (n + 1) · (n + 2) / 2 analyses for evaluation. Hence, for large numbers of uncertain parameters a higher order expansion may become inefficient.

2.2.4 Mean Value Methods

Mean value methods employ most probable point (MPP) analysis, and normally include a first order Taylor series expansion. This class of methods is suitable for well-behaved response functions requiring computationally intensive calculations.[10] The approach is to approximate the probability density function (PDF) rather than creating a metamodel. The outcome is a cumulative distribution function (CDF) of the system response, which can be differentiated to obtain a PDF.

The analysis utilizes a response function Z(**X**) that depends on several random variables **X**. Each point in the design space, spanned by **X**, has a specific probability density according to the JPDF of **X**. Hence, every response value Z(**X**) has a given probability density.[11] The response function is used to define a LSF.

These methods can also provide probabilistic sensitivity measures indicating the input parameters that influence the reliability the most.[12] For more detailed information about these methods refer to the NESSUS Theoretical Manual[13].

2.2.4.1 Limit State Function (LSF)

The failure surface or the limit state, g, for an arbitrary response function Z is defined as:

$$g = Z(\mathbf{X}) - Z_{ls} = 0 \tag{3}$$

where the limit state value Z_{ls} is a particular value of Z. The LSF is defined such that $g(\mathbf{X}) = 0$ is a boundary that divides the random variable space into two regions, failure/infeasible and safe/feasible, see Figure 3.

2.2.4.2 Most Probable Point, MPP

The MPP is the point along the LSF with maximum probability of occurrence, i.e. the point on the LSF where the variable combination yields the highest probability density. For a JPDF of two standard normal and independent variables it is obvious that the point of minimum distance from the origin to the LSF represents the most probable combination of the random variables, and is therefore named the most probable point, as seen in Figure 3. For nonlinear limit states, the computation of this minimum distance becomes an optimization problem. Once the MPP is identified, it can be used as a basis to develop approximate polynomial LSFs.

2.2.4.3 Distribution Transformation

Not always are the random variables of an engineering problem standard normal distributed and independent from each other, which makes the search for a MPP difficult. By transforming variable distributions to independent standard normal, the probabilistic analysis becomes mathematically more tractable. The drawback is that the involved transformation may significantly distort the LSF such that an originally flat surface becomes highly curved. There are several proposed transformation algorithms, suitable for different problems and distributions.[13]

2.2.4.4 The Mean Value Method (MV)

MV is based on a first order Taylor series expansion. Assuming that the response function Z(**X**) is smooth and a Taylor series expansion of Z exists at the mean values $\boldsymbol{\mu}$ of the random variables **X**, the Z-function can be expressed as:

$$Z(\mathbf{X}) = Z(\boldsymbol{\mu}) + \sum_{i=1}^{n} \left(\frac{\partial Z}{\partial X_i} \right)_{\mu} \cdot (X_i - \mu_i) + H(\mathbf{X})$$

$$= a_0 + \sum_{i=1}^{n} a_i X_i' + H(\mathbf{X})$$

$$= Z_{MV}(\mathbf{X}) + H(\mathbf{X})$$

where the derivatives are evaluated at the mean values $\boldsymbol{\mu}$ and n is the number of random variables. The MV-function $Z_{MV}(\mathbf{X})$ represents the sum of the first order terms and $H(\mathbf{X})$ represents the higher order terms. The coefficients a_i can be obtained in several ways. Using numerical differentiation, the minimum number of Z-function evaluations required is $n + 1$. Z_{MV} is used to define a LSF, along which the MPP can be identified. Since Z_{MV} is linear and explicit, its CDF can be computed by mapping the probability for several values of Z_{ls}.

Figure 3 shows the LSF of an arbitrary response function Z, i.e. the exact LSF where $\tilde{g} = Z - Z_{ls} = 0$, and the MV approximated LSF, i.e. $g = Z_{MV} - Z_{ls} = 0$. The random variable space is spanned by two independent standard normal variables.
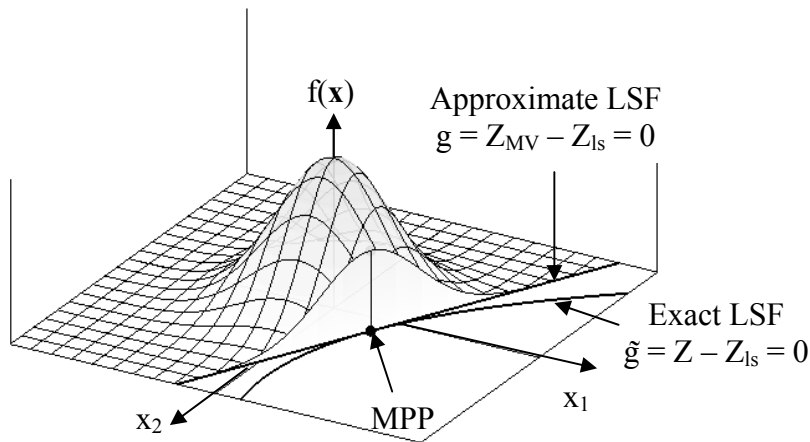
Figure 3   *JPDF f(x) of two standard normal variables. The MV approximate LSF is used to define the infeasible region of the variable space, from which the JPDF has been cut off. Also plotted are the exact LSF and the MPP.*

For nonlinear Z-functions, the MV solution may not be sufficiently accurate. One possible improvement can be obtained by increasing the order of the Taylor series expansion. However, for a computationally expensive process and/or in case of a large number of random variables, this may not be an attractive solution. A more efficient approach is the Advanced Mean Value method (AMV).

2.2.4.5   The Advanced Mean Value Method (AMV)

AMV improves MV by using a correction procedure to compensate for errors introduced from the truncation of the Taylor series. The AMV model is defined as:

$$Z_{AMV} = Z_{MV} + K(Z_{MV})$$

$K(Z_{MV})$ is defined as the difference between Z and Z_{MV} at the Most Probable Point Locus (MPPL) of Z_{MV}, where the MPPL combines the MPPs for several values of Z_{ls}.

The key is reduction of the truncation error by replacing the higher order terms, H($\mathbf{X}$), in the first order expansion to derive Z_{MV}, by a simplified function $K(Z_{MV})$. To update the MV CDF, computation of the Z-function is performed at selected CDF values using the MPPs from the Z_{MV} calculation. As a result of the approximation, the truncation error is not optimum. However, because the MV generated MPPs are generally close to the exact MPPs, the AMV solution provides a reasonably good estimation for many engineering problems.

AMV can provide information on non-linearity of the LSF to detect potential numerical problems. However, AMV calls for additional Z-function evaluations compared to MV. The minimum required number of evaluations is n + 1 + m, where n is the number of random variables and m is the number of CDF levels used for the correction of the MV CDF.

2.3   Correlation, Linear Dependence

In most engineering problems, the values that an attribute variable attains may be dependent on one or more random variables. The linear relation between multiple variables is called covariance, denoted Cov(X,Y) for two random variables X and Y. The correlation coefficient ρ is the covariance non-dimensionalized by the product of the standard deviations of the random variables.

$$Cov(X, Y) = E(XY) - E(X)E(Y)$$

$$\rho = \frac{Cov(X, Y)}{\sigma_X \cdot \sigma_Y}$$

The correlation coefficient ρ ranges between -1 and 1, where 1 indicates perfect positive linear dependence, i.e. Y increases as X increases. Negative linear dependence indicates that Y decreases as X increases. If there is no linear dependence, the correlation coefficient is expected to be zero.

Generally, perfect linear dependence or independence is rare. Hence, two random variables are considered statistically independent or uncorrelated if the correlation coefficient is between +/-0.3 and perfectly correlated for coefficient values over 0.9 or less than -0.9.[5,14]

The characteristics of the relationship between two random variables are visualized with scatter plots as shown in Figure 4. Figure 4.1 shows no relationship at all between the two random variables; consequently the correlation coefficient is zero. In Figure 4.2 there is perfect negative linear dependence ($\rho = -1$). Positive linear dependence is indicated in Figure 4.3, but not perfect. Hence, ρ is expected to be greater than 0 and less than 1. Figure 4.4 shows a strong relationship between the two random variables, but since the relationship is nonlinear, the correlation coefficient is zero.
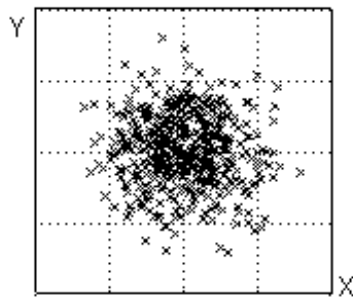
4.1 Uncorrelated random variables, $\rho = 0$.
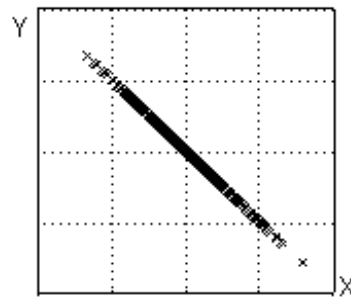
4.2 Perfect negative correlation, $\rho = -1$.
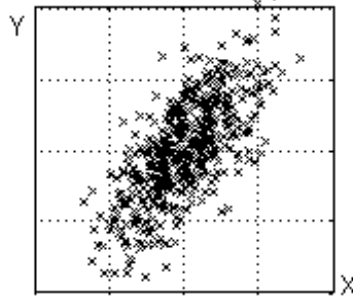
4.3 Not perfect positive correlation, $\rho = 0.68$.

4.4 Non-linear correlation, $\rho = 0$.

Figure 4 *Correlation of two normal distributed random variables.*

3   CONFIDENCE OF SUCCESS CALCULATION

Calculation of CoS in this work is done utilizing MV, leaving out the CDF construction of the AMV and yielding only one specific probability value for each DP. This approach omits evaluating variance or sensitivit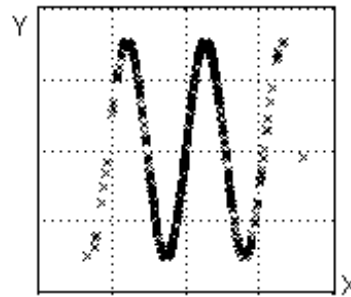y explicitly and focuses only on the probability of meeting predictions, i.e. fulfilling requirements and performance expectations.

For the CoS calculation suggested, there is no need to separately evaluate the correlation between any variables, on a global or local basis. It is taken into account within the calculation for every individual DP, with the exception of nonlinear correlations. However, the usage of the suggested approach calls for close to linear responses locally within the design space, which leads to linear dependence between criteria. This dependence is taken into account by applying the LSFs from any number of criteria, to the JPDF of all uncertain variables.

An example calculation of CoS is shown below, with two standard normal distributed random variables, x and y, and two criterion functions.

An approximate response function Z_{MV} is derived via a first order Taylor series expansion linearized at the mean values of the random design variables. This calls for three system evaluations to calculate the coefficient vector A. (In the present application, each system evaluation is one converged ship design.)

$$\mathbf{Z} = \mathbf{X} \cdot \mathbf{A} \qquad (4)$$

$$\begin{bmatrix} z_0 \\ z_1 \\ z_2 \end{bmatrix} = \begin{bmatrix} 1 & x & y \\ 1 & x+\Delta x & y \\ 1 & x & y+\Delta y \end{bmatrix} \cdot \begin{bmatrix} a_0 \\ a_1 \\ a_2 \end{bmatrix}$$

yielding

$$Z_{MV}(x,y) = a_0 + a_1 \cdot x + a_2 \cdot y$$

Any number of response functions can be approximated in the same manner without any additional system evaluations. All that is required is an evaluation of each response function at each system evaluation (design point).

Figure 5 shows the response surfaces for two arbitrary functions:

$$f_1(x,y) = 5x + 2y + \frac{y^2}{10} \quad \text{and} \quad f_2(x,y) = x + 5y + \sin(3x)$$

and their respective approximated response planes in the vicinity of $(x,y) = (0,0)$:

$$Z_{MV1}(x, y) = 0 + 5x + 2.01y \quad \text{and} \quad Z_{MV2}(x, y) = 0 + 0.87x + 5y$$

The approximate LSFs are calculated from formula (3):

$$g(x,y) = Z_{MV}(x,y) - Z_{ls} = 0$$

where $Z_{ls} = (8,7)$ represents the limit state values defining the boundary between the infeasible and feasible regions in the design space.
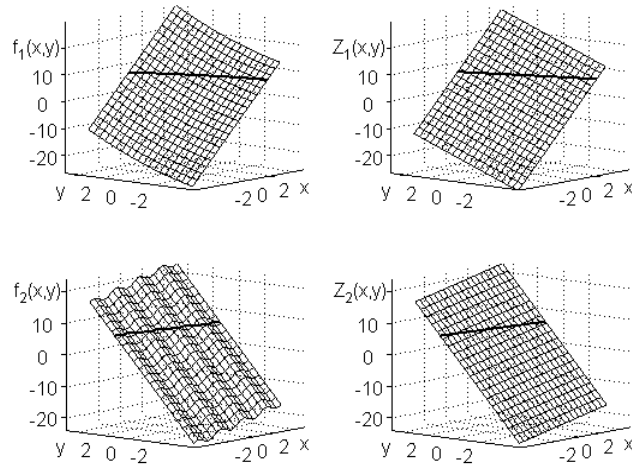
Figure 5 *f_1 and f_2 response surfaces are displayed on the left, and their respective approximated response planes Z_{MV1} and Z_{MV2} are displayed on the right. The bold curves/lines highlight the limit states.*

In Figure 6 the approximate LSFs, g_1 and g_2 with Z_{ls} equal to 8 and 7 respectively, are plotted in the two-dimensional design space. The shaded region shows the part of the design space where $g > 0$, i.e. Z values are higher than Z_{ls}. If $g > 0$ is infeasible, the shaded region represents failing solutions.

Introducing the JPDF of the two random variables, assumed to be standard normal distributed and independent, and applying the LSFs yields the CoS of meeting the requirements, i.e. g less than or equal to 0. Figure 7 shows the JPDF, with the $g > 0$ region (infeasible region) of the function removed. The voulme under the remaining region of the JPDF yields a numerical value of CoS for the specific DP, CoS = 87% in this case.
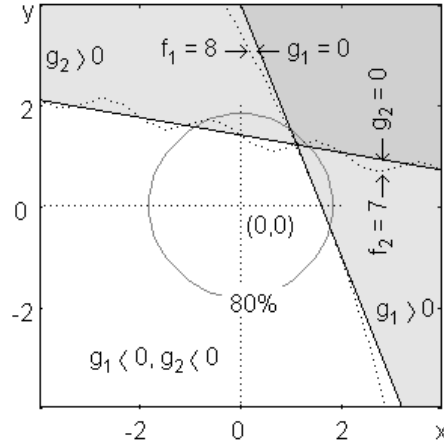
Figure 6 *The design space in the vicinity of the DP; (x, y) = (0 , 0). Solid lines mark the approximate LSFs, while the dotted curves are the actual functions yielding the limit state values. The circle encloses the region where 80% of the distribution is expected for (x, y) Є N(0,1).*
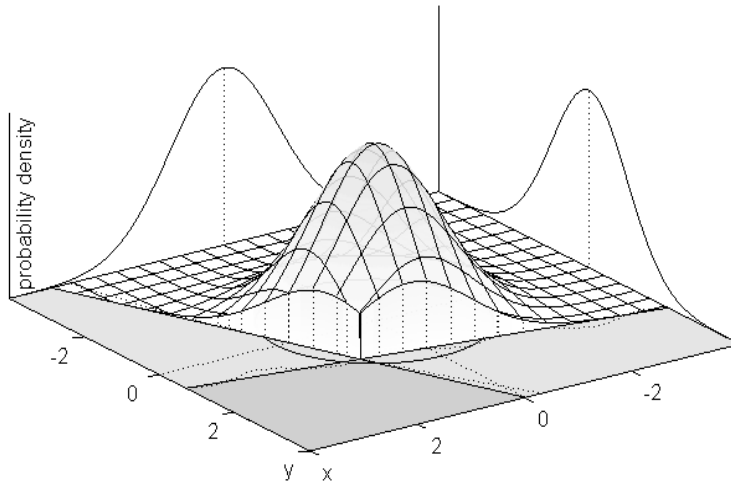
Figure 7 *JPDF of the random variables (x, y) Є N(0,1) reduced by the LSFs. Note that the x- and y-axis are reversed from what was shown in Figure 6.*

Probability in this example and in the demonstration is calculated as a summation approximation of the JPDF f(x,y) integral. The variable space is limited to the interval [-5, 5] for both x and y:

$$1 = \int_{-\infty}^{\infty}\int_{-\infty}^{\infty} f(x,y)dxdy \approx \int_{-5}^{5}\int_{-5}^{5} f(x,y)dxdy \approx 0.999999$$

The variable space is discretized into a large number of small rectangular subintervals. The probability density of each subinterval is calculated at the midpoint of the rectangle, and probability is calculated as the summation of the discrete values:

$$\int_a^b \int_c^d f(x,y)dxdy = \sum_{i=1}^n \sum_{k=1}^m f(x_i, y_k)\Delta x \Delta y \ \text{ when } \ \Delta x, \ \Delta y \to 0$$

where n and m are the number of subintervals in the x and y direction respectively, x_i and y_k are the midpoints of the subintervals i and k respectively, and Δx and Δy are the rectangle subinterval side lengths.

For the CoS calculation, the variable space is discretized into a definite number of subintervals, and the discrete values in the feasible regions, defined by the LSFs, are summed. The subinterval is given a finer mesh in the high density region of each marginal function to reduce the error when the LSFs are close to the variable mean values:

$$\int_a^b \int_c^d f(x,y)dxdy \approx \sum_{i=1}^n \sum_{k=1}^n f(x_i, y_k)\Delta x_i \Delta y_k$$

where n is the number of subintervals, x_i and y_k are the midpoints, and Δx_i and Δy_k are the rectangle side lengths of interval i and k in the x and y direction respectively.

The mesh is generated in a logarithmic fashion in each quadrant of variable space, with 125 intervals in each direction. The finest mesh is located in the corner closest to the mean values. The quadrants are mirrored at the mean values, thus giving a finer mesh in the high density region, as exemplified in Figure 8.
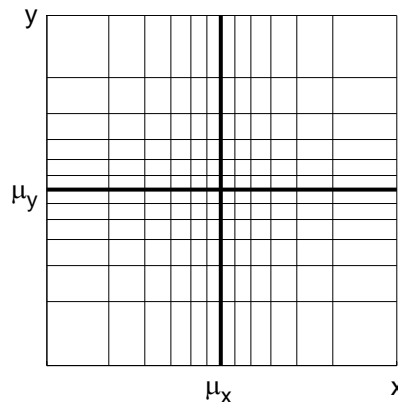
Figure 8 *Logarithmically divided variable space.*

Obviously, there is some correlation of the responses f_1 and f_2 since both functions depend on the x and y variables. A MCS of 100,000 system evaluations is illustrated in Figure 9, showing the marginal PDFs for f_1 and f_2 and their JPDF as a contour plot. The correlation between f_1 and f_2 is evident in the figure.
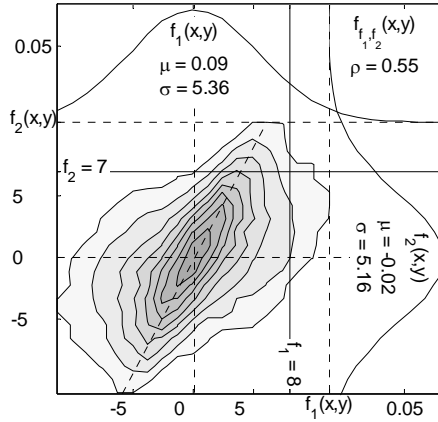
Figure 9   *MCS generated system response JPDF.*

	MCS	CoS
System evaluations	100k	3
$f_1 \leq 8 \cap f_2 \leq 7$	86%	
$g_1 \cap g_2 \leq 0$		87%
ρ	0.55	0.53
$f_1 \leq 8$	93%	
$g_1 \leq 0$		93%
μ_1	0.09	0
σ_1	5.36	5.39
$f_2 \leq 7$	91%	
$g_2 \leq 0$		92%
μ_2	0.02	0
σ_2	5.16	5.07

Table 1   *Comparison of CoS calculation and MCS.*

Table 1 shows the data obtained from the MCS compared with the data from the CoS calculation. The CoS column contains data calculated via a first order Taylor series

approximation only. Correlation, ρ, is also stated for the CoS calculation. Correlation of two variables is simply a measurement of the orthogonality of **g**, i.e. the cosine of the angle between g_1 and g_2 in Figure 6. The mean value, μ, and standard deviation, σ, for each criterion in the CoS column is calculated from the sensitivity based formulae (1) and (2) respectively.

The intended use of CoS does not call for the complete calculation of a CDF. However, since the CoS calculation in this work is merely the first step in creating a CDF with MV, a Joint CDF (JCDF) can easily be obtained. This JCDF should be a good estimate of the empirical JCDF generated from a MCS, verifying that correlation between the functions f_1 and f_2 is covered within the CoS calculation. Figure 10.1 shows a contour plot of a MCS generated JCDF, and Figure 10.2 shows a MV generated JCDF of the two functions.
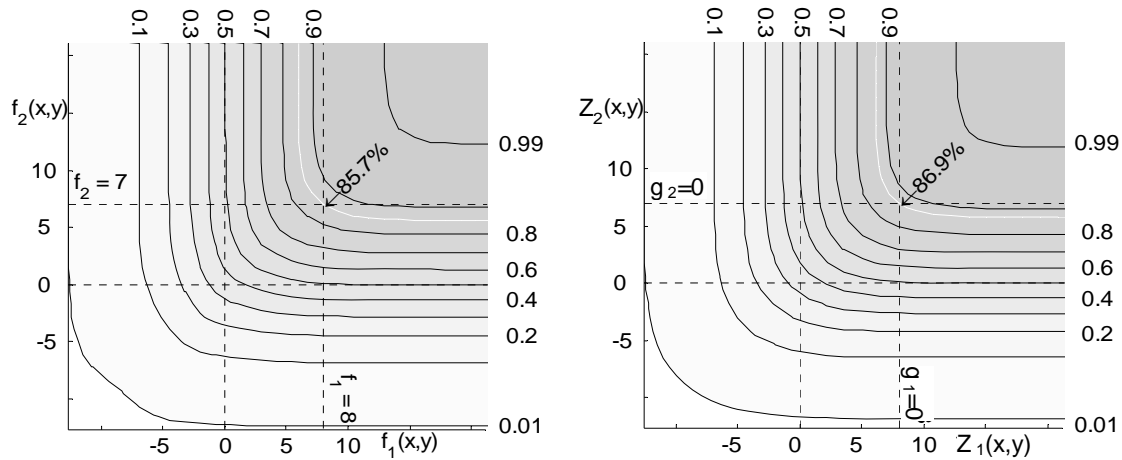
Figure 10.1, *left   JCDF generated via MCS; 85.7% yield $f_1 \leq 8 \cap f_2 \leq 7$*.
Figure 10.2, *right MV generated JCDF; 86.9% yield $g_1 \cap g_2 \leq 0$*.

If such functions as in this example or worse are found in a real system, one should utilize the CoS calculation as suggested in this paper with caution. Nevertheless, the CoS approximation in this example is quite accurate. The maximum absolute difference between the MCS and MV generated JCDFs for this system at this DP is less than 2%. Figures 11 and 12 display the absolute and relative errors between the MV calculation and the MCS calculation.

Some of the error clearly originates from the linearization of the response functions. Depending on the shape of the actual response function, the error caused by the linearization could be expected to increase with increasing distance from the expansion point, i.e. the deterministic DP, which is also where the random variables take their mean values,. However, since the probability becomes less dense with increasing distance from the mean values (for normal distributed variables), the absolute error does not increase

unrestrained; on the contrary the absolute error principally decreases in this example. Also, it should be noted that MCS is also an approximation with associated errors. Thus, in some aspects, the CoS calculation may be closer to the truth than the MCS calculation. The region with the highest absolute error is located close to the deterministic DP, and the DP itself $(x,y) = (0,0)$ yields an error of just under 2%.
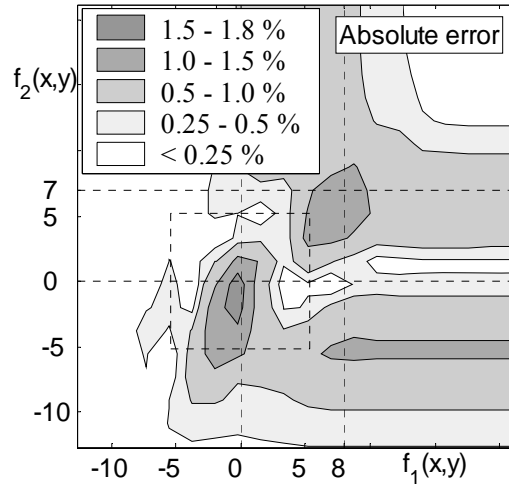
Figure 11 *Absolute difference between MCS and MV JCDFs. The dashed square is enclosing the region for which the response deviation is within σ for each*
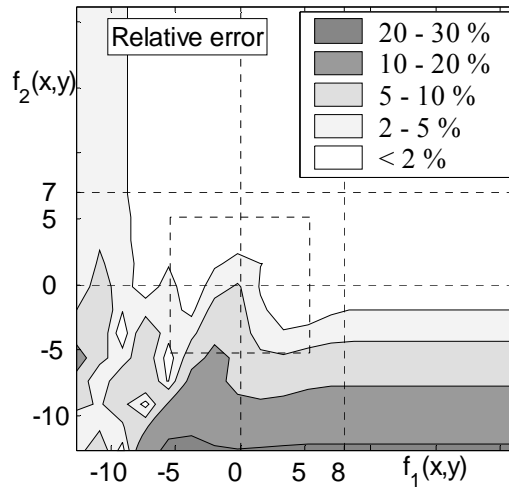
Figure 12 *Error in the MV calculated JCDF relative to the MCS calculation.*

The relative error is greater in the region of low cumulative probability, as could be expected studying the absolute error. Even a small absolute error triggers a huge relative error in this region. Above the 50% JCDF level the relative error never exceeds 2%. The most interesting point is where the two LSFs intersect: $(f_1, f_2) = (8, 7)$ or $(x, y) = (1.11, 1.21)$. The accuracy of the JCDF value at this point is an important indicator of the accuracy of the CoS calculation. The absolute error here is 1.2% and the relative error is 1.4%.

4   DEMONSTRATION SETUP

Implementation of CoS is demonstrated in an optimization of a simplified multi-disciplinary ship synthesis model. Hardware used is a twin-processor Dell PSW650: Xeon 2x2.66 GHz CPU, 1.0 GB RAM.

Figure 13 is a flow chart showing the optimization process for the complete demonstration setup. The ship model components are gathered into one "black box" block, while the other blocks show actual individual system components. If the deterministic constraints reveal a DP is infeasible, CoS is set to zero and no iterations or other computational work is done before the optimizer evaluates the model response.
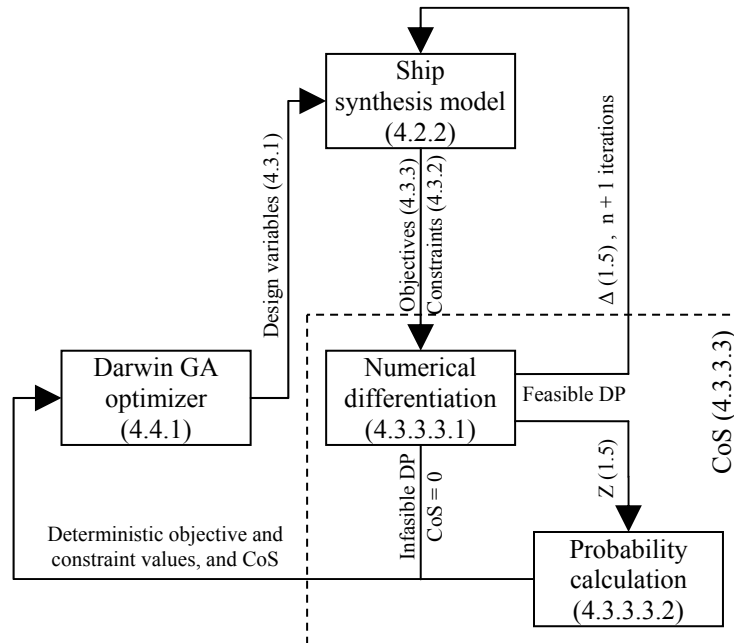
Figure 13   *Flow chart of the demonstration setup. Referring sections are in brackets. It should also be noted that n is the number of random variables.*

4.1   ModelCenter

The simulation tool used in this effort is ModelCenter version 6.0.3 developed by Phoenix Integration, Inc. It is a commercial process integration and design optimization software package, providing a visual environment for integrating applications and codes in order to perform multi-disciplinary design and analysis. Once these codes are placed in

ModelCenter, key data is linked from one application to another, creating an automated design environment.

4.2 <u>Ship Model</u>

The multi-disciplinary ship synthesis model used is and has been under development at AOE VT for several years.[15] In this work the model is attuned to resemble the design of a modern US Navy destroyer. The DDG51 Arleigh Burke has been used as a model evaluation DP and initial design in the optimization effort.

4.2.1 Arleigh Burke Class, Multi-mission Guided Missile Destroyer

The Arleigh Burke class is an all-steel construction designed to operate independently or as units of carrier strike groups, expeditionary strike groups, and missile defense action groups in multi-threat environments that include air, surface, and subsurface threats. These ships will respond to low-intensity conflict/coastal and littoral offshore warfare scenarios as well as open-ocean conflict providing or augmenting power projection, forward presence requirements, and escort operations at sea. The combat systems center around the AEGIS Combat System (ACS) and the SPY-lD multi-function phased array radar, and consist of the vertical launching system (VLS), anti-air warfare (AAW), anti-submarine warfare (ASW), and anti-surface warfare (ASuW).

4.2.2 Synthesis Model Components

The ship synthesis model is made up of several interlinked components, each handling specific calculations, e.g. resistance, hull shape, weight, and combat systems. This model makes it easy to change, add, or remove components to describe the ship or mission type in question, or usage of formulas of preference. Also, integration software allows calculations from other applications, e.g. CFD and FEM, to be included. All components in this model are coded in Fortran and are briefly described in Table 2.

Each design is balanced through the use of fuel tankage sizing. The resulting design is compared to any functional requirements, e.g. range and stability constraints, etc. Hence, no iterative balancing is performed; each design either fulfills requirements or does not, i.e. is deemed feasible or infeasible. Infeasible designs are penalized causing the optimizer to seek feasible designs.

Component	Comment
Combat	The whole array of weaponry and combat systems
Propulsion	Numerous different propulsion systems of choice
Hull	Calculates basic hull design coefficients
Available Space	The ship design's useable space
Electric	Electric appliances and consumption
Resistance	Holtrop & Mennen resistance calculation
Weight	Total ship weight
Tankage	Volume calculation of required tanks
Required Space	Necessary space for all ship functions
Feasibility	Constraint evaluation
Cost	Total Ownership Cost (CTOC) calculation
OMOE	Overall Measurement Of Effectiveness

Table 2 *Ship synthesis model components.*

4.2.3   Simulating Uncertainty

Randomness is assumed to arise only from the embedded uncertainties in the analysis; consequently all input variables are presumed deterministic for each DP. Only the uncertainties in the resistance and weight calculations are modeled in this demonstration. Each uncertainty, Y, is modeled by introducing an extra random variable, X, such that:

$$Y = \mu_y \cdot (1 + \delta \cdot X) \qquad (5)$$

where $X \in N(0,1)$ and is independent of any other random variable. δ is the assumed coefficient of variation, and μ_y is the mean value, i.e. the deterministically calculated value of the parameter at hand.

4.2.3.1   Bare Hull Resistance Prediction

The resistance calculation is performed utilizing the Holtrop & Mennen method. This method is an approximate power prediction method based on statistical data and is thus an obvious source of uncertainty. The standard deviation for the actual bare hull resistance, R_T, is assumed to be 10%, i.e. $\delta = 0.1$.

4.2.3.2   Total and Subsystem Weight Calculation

Apart from summarizing the weight of all subsystems and calculating the light ship weight, this component also balances the design by specifying allowable fuel weight and calculates ship stability. Since total weight generally has a close relationship with the price of a ship (more weight leads to higher cost), any uncertainties in the weight

calculation are expected to have a direct noticeable impact on the total cost, especially in this model where the cost is calculated using a weight-based algorithm.

The total weight, W_T, is calculated as:

$$W_T = \sum \mathbf{W}_D + \sum \mathbf{W}_U$$

where $\mathbf{W}_D$ represents the subsystem weights that are considered deterministic, and $\mathbf{W}_U$ represents the subsystem weights considered to be uncertain. Uncertainty is introduced into the weights $\mathbf{W}_U$ as:

$$\mathbf{W}_U = \boldsymbol{\mu}_{wu} \cdot (1 + \delta \cdot X)$$

where $\boldsymbol{\mu}_{wu}$ represents the mean (deterministic) values of the uncertain subsystem weights, $\delta = 0.1$, and $X \in N(0,1)$.

The weight deviation is thus equitably divided among the summarized subsystem weights that are considered uncertain, which are then passed to the subsequent analyses. Each uncertain subsystem weight is distributed with the same variable X. The total weight, W_T, does not have the same coefficient of variation throughout the design space since the $\sum \mathbf{W}_D / \sum \boldsymbol{\mu}_{wu}$ ratio is not constant.

4.3 <u>Model Attributes</u>

The characteristics of the ship synthesis model are more intricate than presented in this and prior sections. Described here are merely the inputs and outputs used in this work and the additional components used for optimization and CoS evaluation. For further information about the ship model itself and its potential, turn to Dr Alan Brown et al. at AOE VT.

4.3.1   Design Parameters and Variables

There are 47 input parameters, listed in Appendix 1, defining the ship design. Of these, the optimization algorithm uses 24 parameters as design variables, 15 discrete and 9 continuous, in the search for the Pareto optimal set. The design variables are listed in Table 3. Discrete design variables are, for example, combat and propulsion systems, while the ship length, beam and draft are continuous. The remaining parameters are fixed at values appropriate to the DDG51 DP.

Each discrete choice is associated with several parameters describing the characteristics of the feature the variable at hand is simulating. For example, Psys is the propulsion system variable. It specifies the weight, power, fuel consumption, etc. of the main engine(s), as well as the number of propulsors, transmission, and shaft weight, etc.

Variable		DDG51	unit	min	max	type
B	Waterline beam	18	m	9	27	continuous
Cp	Prismatic coefficient	0.615		0.51	0.72	continuous
Cx	Section coefficient	0.822		0.72	0.93	continuous
D10	Hull depth at station 10	12.7	m	6	19	continuous
Lwl	Waterline length	142	m	118	166	continuous
T	Draft	6.1	m	3	10	continuous
TS	Stores duration	60	days	60	90	continuous
VD	Deckhouse volume	5437	m^3	1000	6500	continuous
Ve	Endurance speed	20	knots	20	40	continuous
BALtyp	Ballast type	1		0	1	discrete
CDHmat	Deckhouse material type	1	steel/alu	1	2	discrete
Gsys	Generator system	3		1	4	discrete
NCPS	Collective Protection System	2		0	2	discrete
Nfins	Pair of fins	0		0	1	discrete
Psys	Propulsion system	6		1	15	discrete
AAW	Anti-Air Warfare system	2		1	4	discrete
ASuW	Anti-Surface Warfare system	2		1	2	discrete
ASW	Anti-Submarine Warfare system	1		1	5	discrete
C4I	C4 and Intelligence system	1		1	2	discrete
MCM	Mine Counter Measures	3		1	3	discrete
NSFS	Naval Surface Fire Support sys.	2		1	3	discrete
SEW	Space and Electronic Warfare	1		1	3	discrete
STK	Strike Warfare system	2		1	2	discrete
VLS	Vertical Launching System	2		1	4	discrete

Table 3 *Ship model design variables. The final nine design variables are combat system related and have a large influence on OMOE.*

4.3.2 Constraints

Constraint evaluation is performed in the Feasibility component of the ship synthesis model. Infeasibility is defined as a violation of any constraint and results in a negative error value for the specific constraint. The error in the case of a lower boundary (parameter ≥ constraint) is calculated as:

$$\text{error} = \frac{\text{parameter value - constraint value}}{\text{constraint value}}$$

There are eight constraints, listed in Table 4, of which four are dynamic and four are static design parameters.

Parameter	Constraint	Type	Boundary
TA	Total arrangeable area	min	dynamic
DA	Deckhouse area	min	dynamic
VS	Sustained speed	min	28 knots
KW	Generator power	min	dynamic
GMmin	Min GM to beam ratio	min	0.05
GMmax	Max GM to beam ratio	max	0.15
D10	Hull depth at station 10	min	dynamic
E	Endurance range	min	3500 NM

Table 4 *Ship model design constraints.*

4.3.3   Objectives

The main objectives are low ownership cost and high effectiveness. The CoS objective is added to assure that the ship design is reliable and robust in the sense that it fulfills requirements when built and is as effective and economical as predicted.

4.3.3.1   Total Ownership Cost (CTOC)

A simple weight-based algorithm is utilized to calculate the ship building cost. Also included in CTOC are lifetime operational and systems acquisition costs as well as monetary and other financial effects.

4.3.3.2   Overall Measurement Of Effectiveness (OMOE)

The OMOE function includes important ship performance attributes, such as sustained speed, endurance, signatures, and combat capability. Each attribute is weighted in terms of its relative influence on the system effectiveness according to the specific mission/ship type at hand. There are 21 performance attributes in the OMOE evaluation, and their influence ratios are based on expert opinion[15] (See Appendix 2). The OMOE value ranges between 0 and 1, with 1 being the theoretical most effective solution. In practice there may not be any feasible design even close to 1.

Nine performance attributes originate directly from combat systems, and their relative influence on OMOE is almost 65%. The combat system variables affecting OMOE can be reviewed in Table 3. Remaining attributes affecting OMOE are: endurance range, stores duration, sustained speed, seakeeping, number of shafts, structural vulnerability, collective protection system, infra red signature, acoustic signature, topside radar cross section, and magnetic signature/degaussing.

4.3.3.3   Confidence of Success, CoS

The computation of CoS is divided into two steps, a numerical differentiation and then a probability calculation. To speed up the optimization process, there is no CoS calculation done for deterministically infeasible DPs. In theory, it is possible to get a CoS value close to 50% even for an infeasible DP. However, it is unlikely that any decision maker would strive for an initially infeasible design.

4.3.3.3.1   Numerical Differentiation

This component obtains the criteria responses $\mathbf{Z}$ in equation (4) associated with a preset Δ for each random variable. It is coded in Visual Basic script (See Appendix 3). The user interface, shown in Figure 14, allows the user to choose the Δ-step of the variable at hand. Δ is configured to represent σ for a $N(0, \sigma)$ variable. In the demonstration, the Δ-step is set to 1 for all random variables in use, i.e. $\Delta = 1$ yields $Y = \mu_y \cdot (1 + \delta \cdot 1)$ for equation (5).

distVariable	Step	
Model.SCInput.distResist	1	
Model.SCInput.distWeight	1	

distResponse	Limit state...	Over (1) / under (0)
Model.SCCost.CTOC	0.05	1
Model.SCOMOE.OMOE	-0.05	0
Model.SCFeasibility.Eta	0	0
Model.SCFeasibility.Eda	0	0
Model.SCFeasibility.Evs	0	0
Model.SCFeasibility.Ekw	0	0
Model.SCFeasibility.Egmmin	0	0
Model.SCFeasibility.Egmmax	0	0
Model.SCFeasibility.ED10	0	0
Model.SCFeasibility.Ee	0	0

Figure 14 *CoS user interface.*

By choosing a large Δ-step the influence of small fluctuations in an otherwise monotonic response is minimized. However, with greater Δ there may be a greater risk that the response function will be discontinuous and/or highly nonlinear within the Δ-range. Hence, Δ should not be taken in the outer percentiles of the variable distribution since these specific values are unlikely to occur and may not be representative of the greater part of the response function.

In the demonstration, all constraints and the CTOC and OMOE objectives are (initially) used as CoS criteria. The LSF's for each criterion are constructed such that the limit state is expressed as a fraction of the mean (deterministic value) of each criterion, i.e. Z_{ls} is defined relative to μ_{ZMV} in the LSF: $g = Z_{MV} - Z_{ls}$, e.g. $g = Z_{MV} - 1.05 \cdot \mu_{ZMV} = 0$.

Figure 14 shows that the LSF of CTOC is activated at the deterministic value of CTOC plus 5%, while the OMOE LSF is active at the deterministic value of OMOE minus 5%. This means that the decision maker is looking for the design that has the highest probability of not being worse than 95% of the predicted effectiveness and not over 5% more expensive than predicted. By stating 0, Z_{ls} is set to the value zero, which is appropriate for the error functions of the constraints. Further, by typing 1 in the "Over/under" column, g > 0 is considered infeasible. For 0, infeasibility is defined as g < 0.

4.3.3.3.2 Probability Calculation

The LSFs are introduced into the subspace spanned by the random variables to trim their JPDF. The JPDF is simply divided into a finite number of subintervals over the distribution range, limited to +/- 5σ. The portion of the JPDF located in the infeasible region is removed (See Figure 7), and the remaining JPDF subintervals are summed to obtain a numeric CoS value. This component is coded in Matlab (See Appendix 4).

4.4 **Optimization Algorithm**

Optimization is done using a Genetic Algorithm (GA); the Darwin ModelCenter plug-in.

GAs use models of natural selection to improve a population of individuals or variants based on Darwin's principle of survival of the fittest - evolution. They are particularly useful for problems involving discrete variables. These algorithms are also ideally suited to optimize discontinuous and disjointed functions.[15] A major advantage of this type of algorithm is the high probability of locating the global optimum, not just one of the local optima.[4]

The evolutionary process is simulated by the creation of a population of individuals (specific designs) represented by chromosomes (design variable vectors). A population is usually produced from a previous generation through mutation and reproduction. Mutation is alternation of the genes (one design variable or subsets of the design vector) of one individual to create a new individual, while reproduction produces a new individual by combining genes from two (or possibly more) parents. Each individual within the population is evaluated for its fitness, i.e. how well it performs and fulfills requirements. Each new population is referred to as a generation.

4.4.1 The Darwin Optimization Tool

Darwin version 1.1.2 is a GA-based optimization tool, used as a ModelCenter plug-in, designed specifically for solving "real world" engineering optimization problems. It is capable of solving multi-objective design problems with any number of constraints, and it is well suited for discontinuous, noisy, and/or multi-modal design spaces. The plug-in features a GUI that allows the user to relatively quickly define the design problem, and several algorithm variables can also be specified to control the evolutionary process.

5   DEMONSTRATION RESULTS

The applicability and usability of the CoS calculation is explored by implementation in the optimization process of the ship synthesis model described in the preceding section. Before the initial optimization, an examination of the model response is performed. Concluding this section is a second optimization with some alteration to the CoS criteria.

5.1 Model Response Examination

As discussed earlier, in order to get good results from the CoS calculation, the criteria response has to be almost linear and/or concentrated to the mean performance value. Of course, over the whole design space of a complex ship model no response function can be expected to be even close to linear.[15] However, locally in close vicinity to a DP, there is definitely a good chance of a continuous, well-behaved response. If the response is also almost linear and has low variance, there is nothing to discourage calculating CoS as suggested in this paper. To learn criteria response behavior, a few deterministically feasible DPs were randomly selected and evaluated via a short sample MCS (100,000 system evaluations).

All DPs yield an almost perfect linear response for CTOC as well as the TA, GM min, and GM max constraint error values (see Table 4). The exceptions are the sustained speed and endurance range error values, both of which are noticeably non-linear but continuous, and OMOE, which is discontinuous. The DA, KW, and D10 error values are not a function of the RVs. Presented in Figure 15 are some of the criteria response surfaces for the DDG51 DP, namely the objectives CTOC (Figure 15.1) and OMOE (15.2), and the endurance range constraint error values for E (15.3) and VS (15.4) as functions of bare hull resistance, R_T. and total weight, W_T.

The relatively well-behaved responses of the constraints and the CTOC objective indicate that a first order Taylor series expansion should be satisfactory to approximate the response functions in close vicinity to any DP.

The shape of the OMOE response is somewhat discouraging. Although the response seems to have the same general form throughout the design space, there are differences in plateau shape, size, and position for each individual DP. A first order Taylor series expansion will have significant problems approximating a response plane to this shape. However, for the demonstration, OMOE will initially be kept among the CoS criteria. The effect of the OMOE response on the CoS calculation will be further discussed in Section 5.2.3 Evaluation of Confidence of Success Calculation.

29
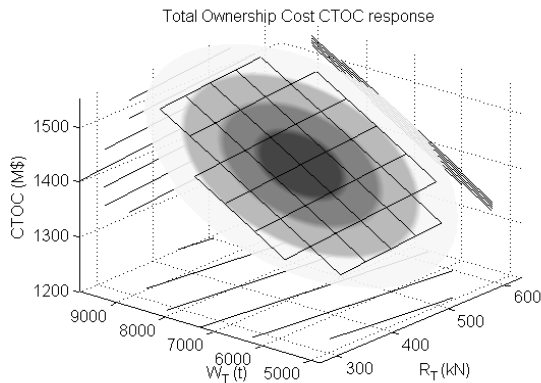
15.1 *CTOC response.*
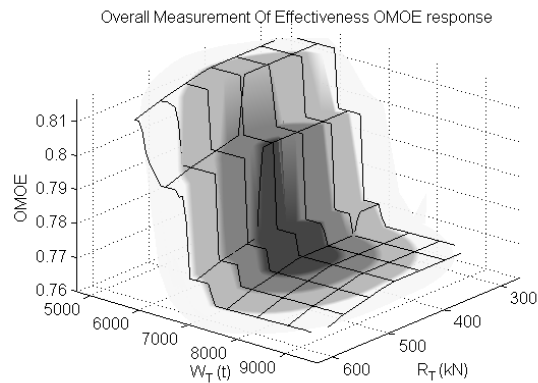
15.2 *OMOE response.*
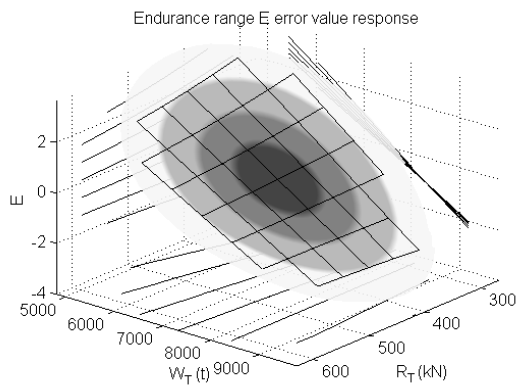
15.3 *E constraint error value response.*
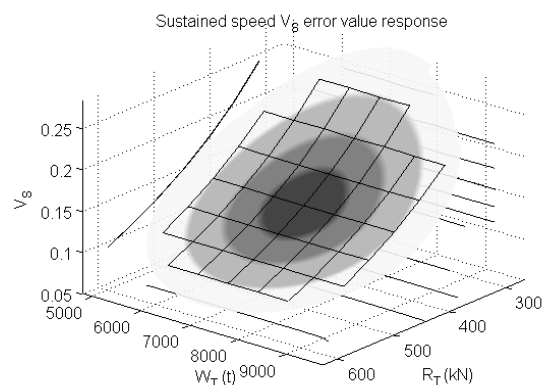
15.4 *VS constraint error value response.*

Figure 15   *Criteria responses in RV space for the DDG51 DP. The mesh size is σ for both R_T and W_T. The darker region of the response surface indicates a higher probability of occurrence.*

Except for OMOE and those constraints that are not a function of the RVs, CoS criteria distributions are more or less Gaussian. The CTOC - OMOE joint distribution from the MCS of the DDG51 DP is plotted in Figure 16. Notice that the OMOE and CTOC objectives are not conflicting here in the sense that a lower CTOC corresponds to a higher OMOE, even though they are conflicting in the global optimization where low CTOC results in a low OMOE. This is because a lower than deterministic weight at a specific DP results in both a less expensive and more effective ship, as can also be observed by studying Figures 15.1 and 15.2. The endurance range error value distribution is shown in Figure 17.

Figure 16 *Joint distribution of the objectives CTOC and OMOE for the DDG51 DP.*
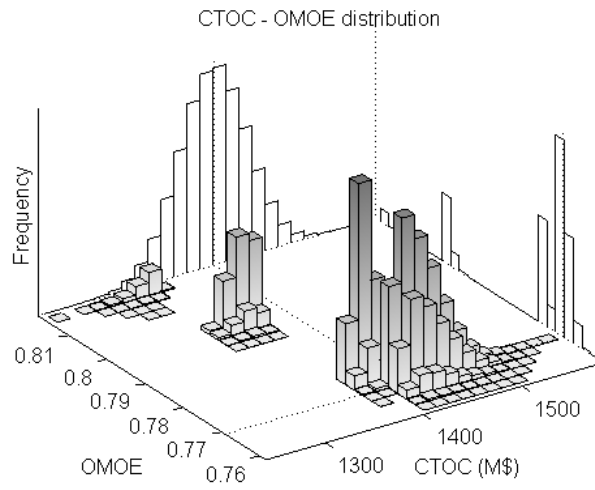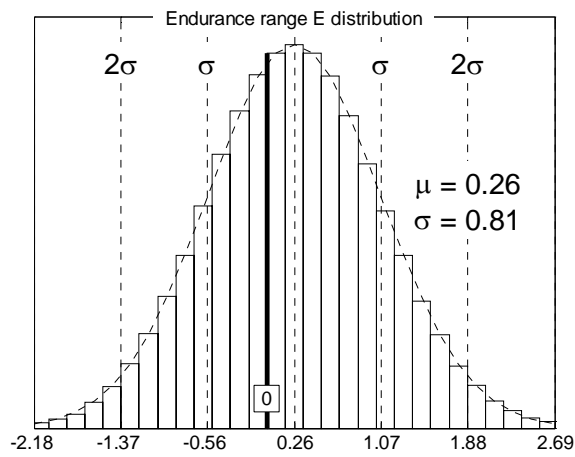

Figure 17 *Distribution of the E constraint error value.*

A full calculation of CoS is performed for the DDG51 DP and compared with a MCS in Table 5. The resemblance is good with a maximum difference of 0.13% for the GMmin constraint and an overall CoS error of 0.03% compared to MCS.

A more illustrative presentation of Table 5 is produced by overlaying the MCS distribution with the approximated LSFs. This gives a visual perspective of the resemblance between the MCS and the CoS calculation. Figure 18 shows the design subspace spanned by the random variables. The subspace is scattered with the solutions generated through the MCS; the feasible solutions are marked with '+' and infeasible with '**x**'. The LSFs from the CoS calculation are overlaid on the scatter plot.

Criterion	MCS (%)	CoS (%)	Error
CTOC	98.25	98.17	0.08
OMOE	100.00	99.99	0.01
TA	95.97	95.99	-0.02
DA	100.00	99.99	0.01
VS	100.00	99.99	0.01
KW	100.00	99.99	0.01
GM min	97.06	96.93	0.13
GM max	99.99	99.98	0.01
D10	100.00	99.99	0.01
E	62.19	62.31	-0.12
CoS	**58.16**	**58.13**	**0.03**

Table 5 *CoS calculation compared to MCS (100k sys. eval.) for the DDG51 DP.*

The LSFs follow the edges of the infeasible regions quite well. Note that the OMOE LSF does not show in Figure 18. It falls outside of the domain of this plot. Also note that the LSFs of the objectives have no influence on the feasibility for this DP. This is because of the acceptance of a 5% increase in CTOC and a 5% decrease in OMOE from the deterministic solution. A tightening of these limits is addressed in 5.2.4 Confidence of Success Criteria Revised.
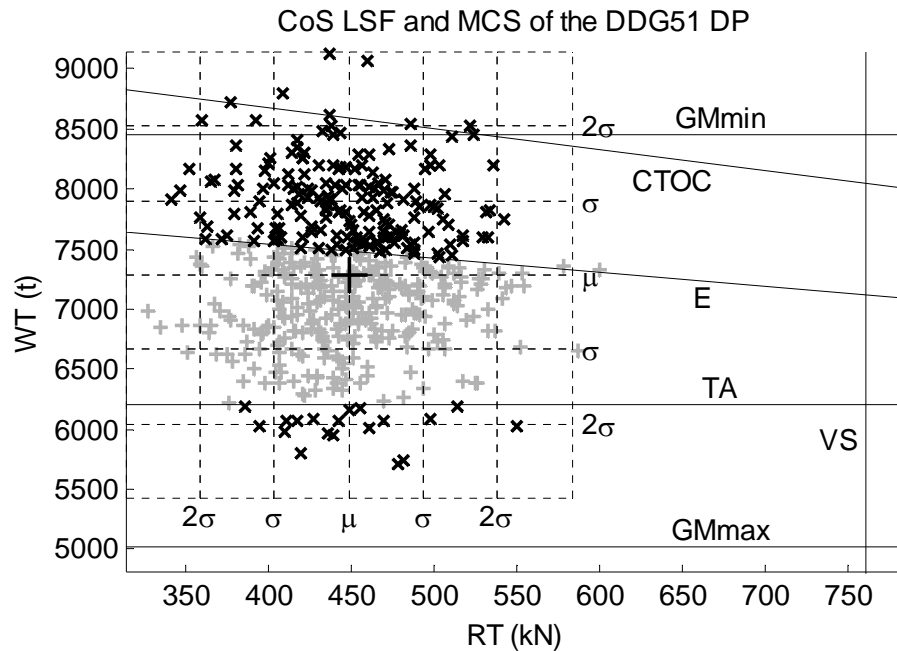
Figure 18 *RV subspace scattered with MCS generated solutions. Feasible solutions are marked with '+' and infeasible with 'x', overlaid with the approximated LSFs of the CoS calculation.*

5.2 **Optimization Implementing Confidence of Success**

The optimization problem is formulated as:

min CTOC(**x**), and
max OMOE(**x**), and
max CoS(**x**)

subject to,

TA(**x**)	$\geq$	TAmin(**x**)
DA(**x**)	$\geq$	DAmin(**x**)
VS(**x**)	$\geq$	28
KW(**x**)	$\geq$	KWmin(**x**)
GM(**x**)	$\geq$	0.05
GM(**x**)	$\leq$	0.15
D10	$\geq$	D10min(**x**)
E(**x**)	$\geq$	3500

where **x** is the DP consisting of 47 design parameters, including D10. The DDG51 DP is used as the initial design, and variable boundaries are set in harmony with the DDG51 design (See Table 3 and Appendix 1). The GA is set to work with a population size of 300 designs per generation and breed/mutate from the 100 best individuals.

5.2.1 Computational Time Expenditure

The optimization stopped after 70 hours or 215 generations due to lack of evolvement. There were a total of 46,079 deterministic infeasible and 18,422 deterministic feasible designs evaluated. CoS was calculated for all deterministic feasible designs, adding another 36,844 evaluations as part of the optimization run as seen in Table 6.

There is a 37% increase in total computational time to complete the three-dimensional objective space optimization because of the extra evaluations called for by the CoS calculation. This increase will be greater if more analyses or variables are considered uncertain. To approximate a response plane, each of the two present uncertainties use about 1.6 seconds every time a feasible DP is encountered, compared to 2.7 seconds for a complete model evaluation. Also, the actual probability calculation adds another 0.3 seconds for each feasible design, which sums up to 1.6 + 1.6 + 0.3 = 3.5 seconds.

	Evaluated Designs	Iterations w/ CoS	Time (hours)	Time w/ CoS	Sec per Design	Sec/design w/ CoS	Time Increase
Optimization	64,501	101,345	48.9	66.9	2.73	3.73	37%
Infeasible	46,079	46,079	34.9	34.9	2.73	2.73	0%
Feasible	18,422	55,266	14.0	31.9	2.73	6.24	129%
CoS	18,422	36,844		18.0		3.51	

Table 6 *Optimization time increase caused by implementation of CoS. The CoS entry emphasizes the effect on the evaluation of feasible designs.*

Assuming each additional uncertain variable would use about the same computational time relative to an evaluation without CoS (excluding the probability calculation which does not increase to any great extent) and that the feasible/infeasible ratio roughly holds, the total time increase of the optimization of the problem at hand can be expected to be approximately a multiplier as tabulated in Table 7. The assumptions are very rough, but the results give an indication that the Taylor series expansion used in the CoS calculation is more efficient in systems with heavy computational burden and a few uncertain variables rather than vice versa.

TIME CONSUMPTION FOR ONE COMPLETE SYSTEM EVALUATION

	2.73 s	5.46 s	13.7 s	27.3 s	137 s	4.6 min	46 min
1	1.2	1.2	1.2	1.2	1.2	1.2	1.2
2	**1.4**	1.4	1.4	1.3	1.3	1.3	1.3
5	2.0	1.9	1.9	1.9	1.8	1.8	1.8
10	3.0	2.8	2.7	2.7	2.7	2.7	2.7
50	11	10	10	10	9	9	9
100	21	19	18	18	18	18	18
1000	200	185	175	172	169	168	168

(Left axis label: NUMBER OF RV)

Table 7 *Increase of computational time caused by the CoS calculation in systems with various numbers of random variables and computational time per evaluation. Highlighted is the case of the system demonstrated.*

5.2.2 Optimization Result Evaluation

The resulting Pareto set is made up of 260 design solutions, graphically presented as a three-dimensional scatter plot in Figure 19. Table 8 presents the best designs for each objective, as if the process had been a single objective optimization. Complete characteristics of the solutions can be found in Appendix 5. The components of the Utopian vector are in bold numbers. Also in Table 8 are the DDG51 and "Best" designs.

A possible method for choosing a "Best" solution from among the Pareto set is to define the "Best" design as the solution that yields the highest objective ratios for all objective combinations concurrently. That is, OMOE/CTOC, CoS/CTOC, and OMOE · CoS are combined into one subjective value, i.e. possibly a good compromise is:

$$\text{Best DP} = \max\left(\frac{\text{OMOE} \cdot \text{CoS}}{\text{CTOC}}\right)$$

Again, this solution may not actually be the "best" solution or preferred design; it is merely one optimal solution among others. As discussed earlier, what design to choose is up to the decision maker and depends on preferences and the shape of the Pareto front. The designs in Table 8 are only elementary solutions presented as guidance.

Solution	CTOC (M$)	OMOE	CoS
CTOC DP	**742**	0.55	0.40
OMOE DP	1394	**0.83**	0.38
CoS DP	1285	0.65	**0.97**
Best DP	967	0.66	0.86
DDG51	1418	0.77	0.58

Table 8   *The performance of various design solutions. The Utopian vector is in bold.*
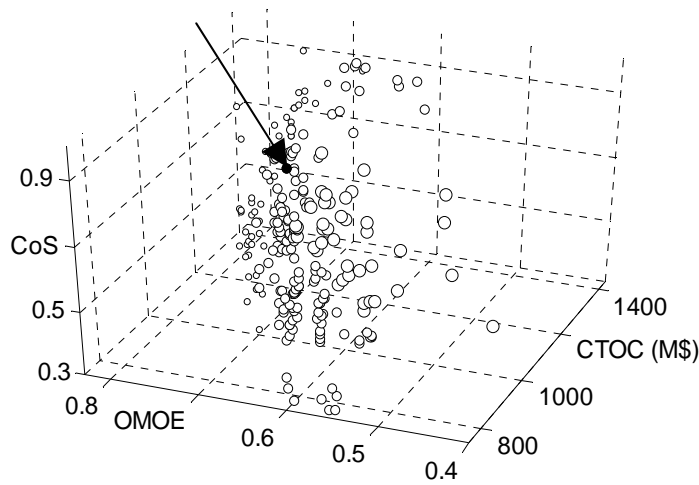
Figure 19   *The objective space scattered with Pareto optimal solutions. The "Best" design from Table 8 can be identified as the black colored solution pointed out by the arrow. This plot is extremely hard to interpret in printed form. The following figures may be more informative.*

A surface fitted to the Pareto optimal set may be somewhat misleading and very hard to translate to specific solutions. More informative can be a Pareto front at every desired level of CoS, i.e. a two-dimensional Pareto front is extracted at the 75% CoS level among all non-dominated designs with CoS ≥ 75%, and a front at 25% is extracted among all designs with CoS ≥ 25%. The gain is that actual solutions form the front instead of a contour derived from an approximate function. Figure 20 shows two-dimensional Pareto fronts at 0%, 75%, and 90% CoS levels in three-dimensional space. Figure 21 shows the corresponding contour plot in CTOC – OMOE space. The 0% CoS frontier is the same Pareto front that would have been found in a deterministic optimization with only CTOC and OMOE as objectives. It is the front determined regardless of CoS.
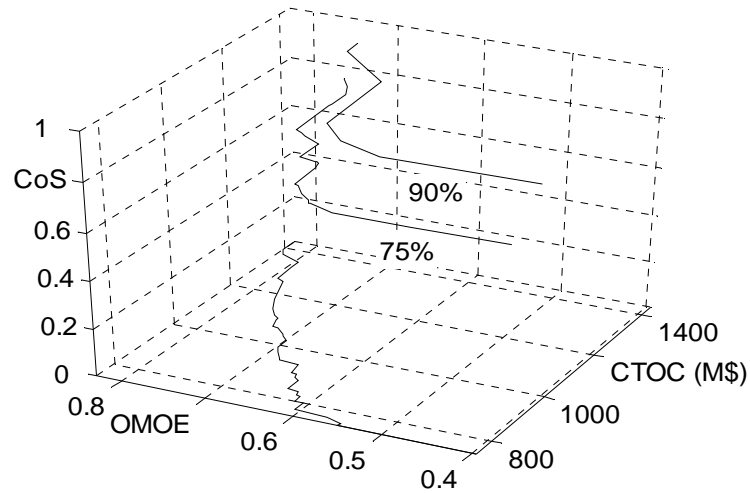
Figure 20   *Pareto fronts at 0%, 75% and 90% CoS levels in 3D objective space.*
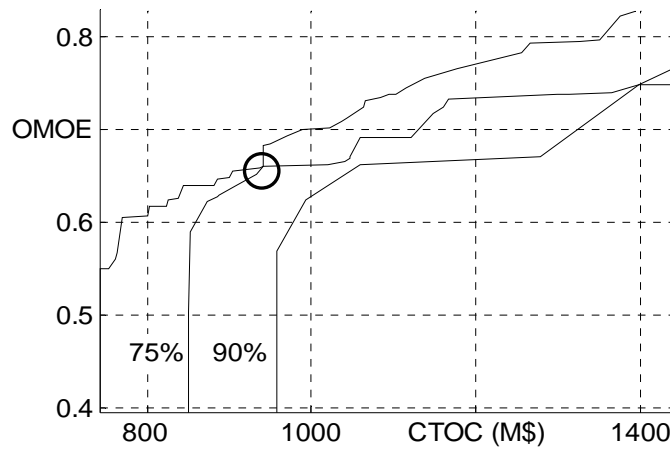
Figure 21   *Contour plot of Pareto fronts at 0%, 75%, and 90% CoS levels. Encircled is where the 0% and 75% CoS Pareto fronts coincide.*

Note that the frontiers in Figures 20 and 21 do not always correspond to feasible designs. Only the actual solutions in the objective space have a feasible representation in the design space. The solutions are connected to visualize the Pareto front. Of course, there might be a feasible design along any line, but if so it has not been found in the optimization process.

Interestingly, the 0% and 75% CoS level frontiers coincide for (CTOC, OMOE) = (941, 0.66), encircled in Figure 21. This means that there is one design defining the 0% CoS

Pareto front that actually has a CoS level of at least 75%. In fact, the CoS value of that design is 0.82, which is the highest CoS of any design making up the 0% CoS frontier. This means a CTOC-OMOE optimization would have found a Pareto front with at least one design that outperforms the DDG51 DP in terms of CoS, even though CoS had not been an objective. The lowest CoS value among the Pareto solutions is 0.28, and the lowest CoS value among all feasible designs is 0.04.

The process of extracting Pareto fronts at different levels among the Pareto optimal designs can obviously be performed for any objective, thus creating a more well-defined surface over a greater region of the objective space. Figure 22 shows Pareto fronts extracted at various levels for each one of the three objectives in the same manner as described for the CoS frontiers above. A surface is applied in Figure 23, providing a more complete description of the Pareto front. The surface color is defined the same way the "Best" DP is identified: brighter color equals a "better" design.
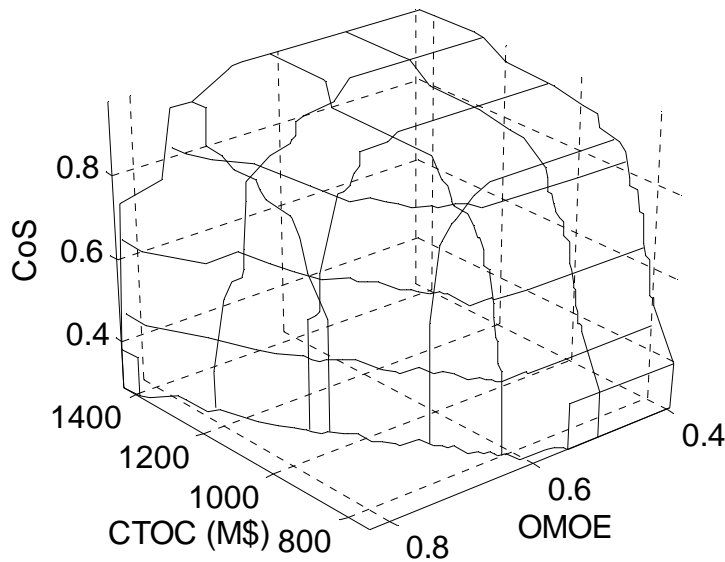
Figure 22 *Wire-frame Pareto surface in three-dimensional objective space. Note that the CTOC and OMOE axes are shifted and that the OMOE axis is reversed.*

The optimization resulted in 260 design solutions that are probably "better" solutions than the DDG51 design. However, if the objective space is reduced to include Pareto solutions that outperform the DDG51 design in all aspects concurrently, i.e. cheaper, more effective, and yielding higher CoS levels, only a few are found. This is mainly because of the relatively high level of effectiveness achieved by the DDG51 design. This is no surprise since the OMOE component focuses on combat system evaluation (See 4.3.3.2 Overall Measurement Of Effectiveness), and the DDG51 design is cramped with modern state of the art weaponry and sensors. There are only two solutions, DP1 and

DP2 in Table 9 and Appendix 5, in this reduced objective space that noticeably outperform the DDG51 DP.
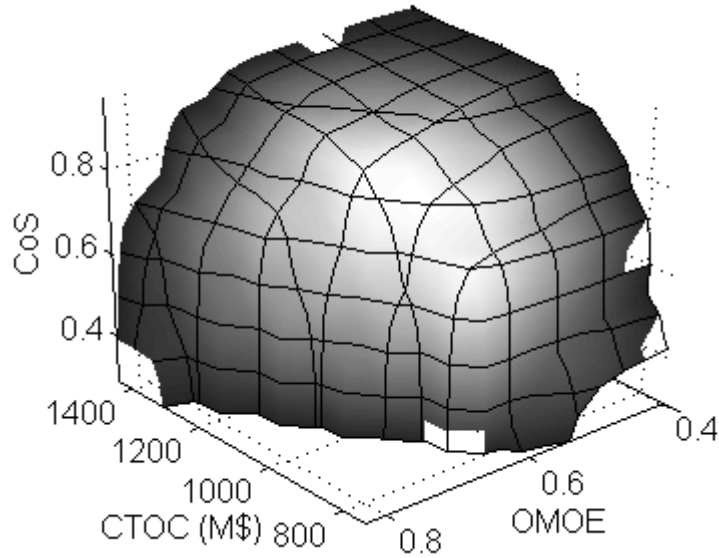
Figure 23 *The Pareto optimal set presented as a surface.*

Solution	CTOC	OMOE	CoS
DDG51	1418	0.77	0.58
DP1	1267	0.79	0.71
DP2	1374	0.82	0.73

Table 9 *Pareto solutions that outperform DDG51 in all aspects.*

5.2.3   Evaluation of Confidence of Success Calculation

To verify that the CoS calculation is performing accurately, the designs from Table 8 and Table 9 are compared with a MCS in the same manner as in Table 5. The probability differences between the MCS and CoS calculation for all criteria and CoS are tabulated in Table 10.

The CoS calculated sustained speed constraint, VS, is failing marginally for the CTOC DP. In this case the VS LSF is close to the bare hull resistance, R_T, mean value and the non-linearity of the VS response takes its toll in the low percentile regions of the total

weight, W_T, distribution. Nevertheless, the CoS value is quite accurate because other LSFs are in effect and thus reduce the overall error.

Criterion	CTOC DP	OMOE DP	CoS DP	Best DP	DP1	DP2
CTOC	-0.13	0.29	0.15	-0.10	-0.06	0.01
OMOE	0.01	0.01	0.01	**8.10**	0.01	0.01
TA	0.01	0.01	0.01	-0.24	-0.05	-0.01
DA	0.01	0.01	0.01	0.01	0.01	0.01
VS	**-1.11**	-0.14	0.02	0.01	0.01	0.01
KW	0.01	0.01	0.01	0.01	0.01	0.01
GMmin	-0.10	0.05	-0.02	0.02	-0.01	0.02
GMmax	-0.01	0.08	-0.10	-0.23	-0.00	0.01
D10	0.01	0.01	0.01	0.01	0.01	0.01
E	0.33	-0.34	0.47	-0.03	0.10	0.83
CoS	-0.38	-0.63	-0.04	**6.02**	0.09	0.84

Table 10 *Probability difference (%) between the MCS and CoS calculation for various Pareto optimal solutions.*

For the "Best" design, CoS is significantly under estimated. This is caused by the OMOE LSF. As seen before in Figure 15.2, the OMOE response is not well-behaved. Figure 24 shows the OMOE function in the vicinity of the "Best" DP. The general shape is not any different than other DPs, but when comparing it to the DDG51 DP, shown in Figure 15.2, it is seen that here the deterministic value falls on the middle plateau rather than on the lower plateau as it did for the DDG51 DP.
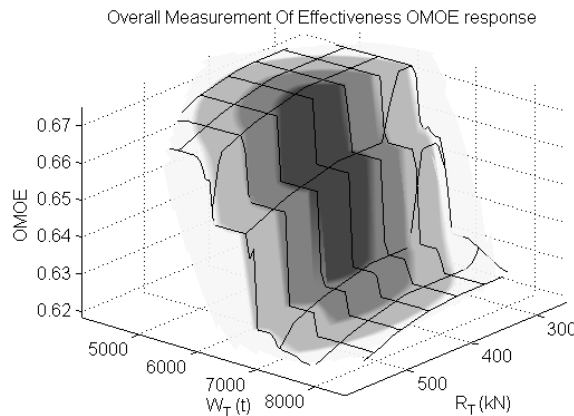

Figure 24 *OMOE response in RV space for the "Best" DP.*

Again, while the approximated OMOE response plane is not good for all DPs, this particular DP is among the worst cases. Figure 25.1 shows the LSFs for the "Best" DP, and Figure 25.2 shows the approximated and exact OMOE LSFs. Note that the approximated OMOE LSF excludes many more designs than does the exact.
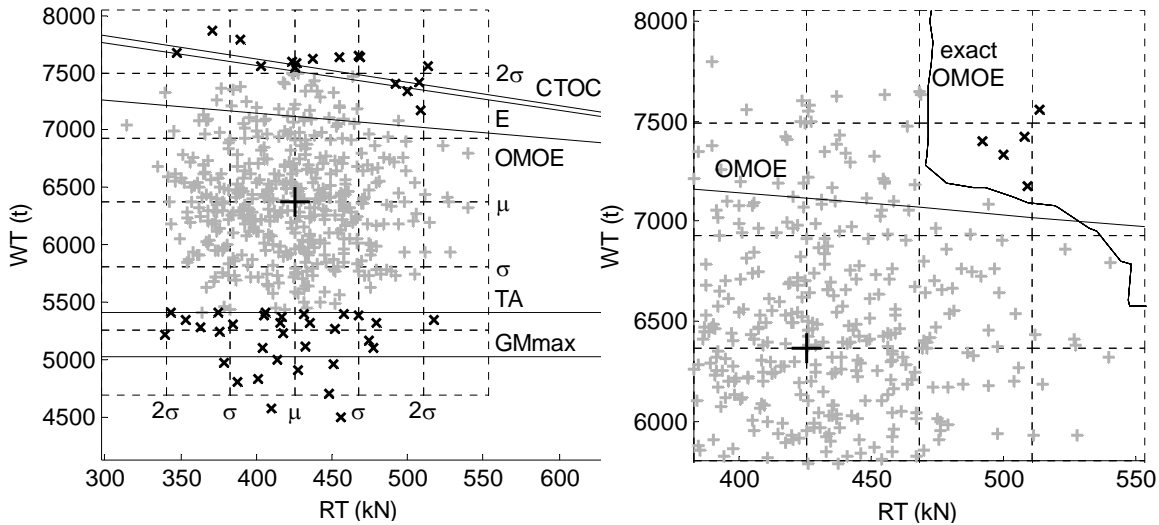
Figure 25.1*, left   CoS LSFs and MCS in random variable space for the "Best" DP.*
Figure 25.2*, right   Exact and approximated OMOE LSFs for the "Best" DP.*

5.2.4   Confidence of Success Criteria Revised

Even though the OMOE LSF does not seem to be in effect for most of the attractive Pareto solutions, there is an obvious risk that the optimization has misinterpreted some solutions of interest because of the bad approximation of the OMOE response. It is quite clear that a function such as OMOE in the demonstration should be handled with care and perhaps should not be used as a CoS criterion. Since the OMOE LSF is not in effect for most of the attractive Pareto solutions, removing the OMOE criterion from the CoS calculation in the optimization of the demonstration model does not change the Pareto front to any great extent. This is because of the acceptance of the somewhat hefty OMOE degradation in combination with the influence of other criteria on CoS. With this in mind, CoS criteria were revised to focus on the confidence of achieving cost (CTOC).

A limit of a 5% increase for CTOC was initially considered as an acceptable deviation from the deterministic value. Whether or not this is an economically justifiable divergence, the outcome of the optimization shows that this limit is rarely in effect. The CTOC distribution generated from the MCS of the DDG51 DP suggests that the 5% limit is about 2σ from the deterministic CTOC value, which might be too loose of a limit. By

reducing the CTOC limit state as much as possible without decreasing CoS for the DDG51 DP, the optimization algorithm is forced to focus on more economically robust solutions compared to the DDG51 design. Reduction of the CTOC limit to 1.2% has a significant effect on the optimization outcome.

Figure 26 shows the Pareto front of a new optimization run, excluding OMOE from the CoS calculation and reducing the acceptable CTOC increase to 1.2%. All other settings were left unchanged. The Pareto optimal set is significantly squeezed in the CoS direction, compared to the original set in Figure 23. The CoS optimal solution, marked with '+' in Figure 26, reaches only 73% CoS. Another difference from the initial run is that the DDG51 DP is among the non-dominated solutions, marked with 'x' in Figure 26. Hence, there are no solutions outperforming the DDG51 DP in all aspects.
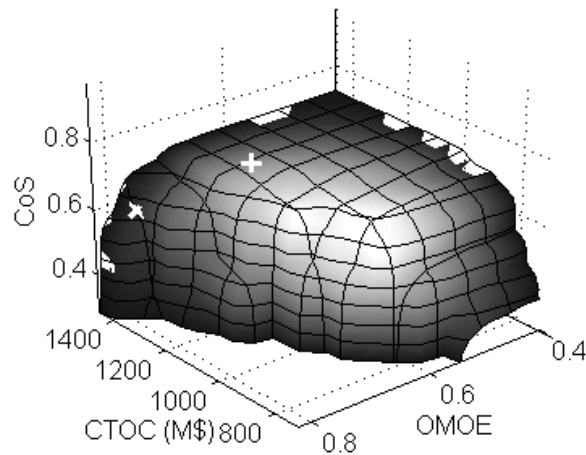
Figure 26   *Pareto front with revised CoS criteria. The DDG51 design is marked with 'x' and the maximal CoS solution is marked with '+' (both are white).*

Since the Pareto optimal set is lacking high CoS value solutions (90%+) and the only significant change made to the model is the CTOC limit, it looks like the design space is unable to provide a solution with low CTOC variance. That is, the genetic algorithm (GA) cannot find a solution that is (much) more cost robust than the DDG51 design.

Even though low CTOC variance is not an aim in the optimization, it is quite natural to presume that at least the solutions with higher CoS values will also exhibit low CTOC variance. In Figure 27 the CTOC coefficient of variance, δ, of all feasible designs found by the GA is contour plotted in CTOC – OMOE objective space. The coefficient of variance, $\delta = \sigma / \mu$, is calculated utilizing the sensitivity based formula, equation 2.

There are almost 17,000 feasible solutions, of which some may coincide in the objective space. There is no guarantee that any coinciding or neighboring solutions yield similar CTOC δ. Figure 27 gives an indication of the general relation between the objectives and

CTOC δ. The trend of increasing CTOC yielding reduced δ is evident. However, it is not possible to single out any obvious favorable region. Marked with 'x' in the upper right corner of Figure 27 is the DDG51 design; this region shows relatively low δ values. In the region with low δ values closer to the center of the plot is the maximum CoS solution, marked with '+'. Even though not totally circumstantial, the plot does not suggest that the CoS solution will be found in this region, only that it is more likely.
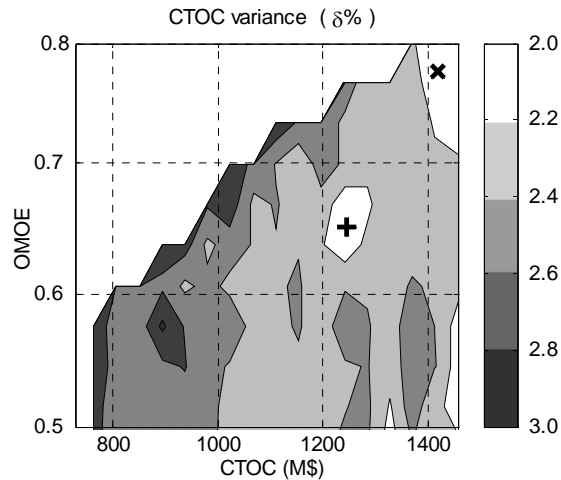
Figure 27   *CTOC variance expressed with δ% for all feasible solutions generated in the optimization process.*

The contour plot in Figure 28.1 covers the CTOC coefficient of variation for the Pareto optimal set only, 280 non-dominated (nor coinciding) solutions. Still, neighboring solutions do not necessarily show similar characteristics, except for the objective values including CoS. With increasing distance from the 0% CoS Pareto front, the GA has clearly favored solutions with low CTOC δ to be able to increase CoS. The 'x' lies within a region more accurately reflecting the actual CTOC δ of the DDG51 design, which is just below 2.4%. Also shown in Figure 28.1 is the probability of CTOC meeting expectations. According to the probability levels, it looks like there might be a good chance of achieving high CoS values in, for example, the vicinity of (CTOC, OMOE) = (1400, 0.72). This region yields at least 72% probability in meeting CTOC expectations.

Figure 28.2 shows the reliability of the objective space, i.e. it compiles the probability of fulfilling constraint requirements for the constraint having the lowest such probability (worst case) for each solution. The most reliable solutions, 93 – 97% fulfillment probability, can be found in the region around (CTOC, OMOE) = (1050, 0.62). Reliability around (1400, 0.72) is over 84%.
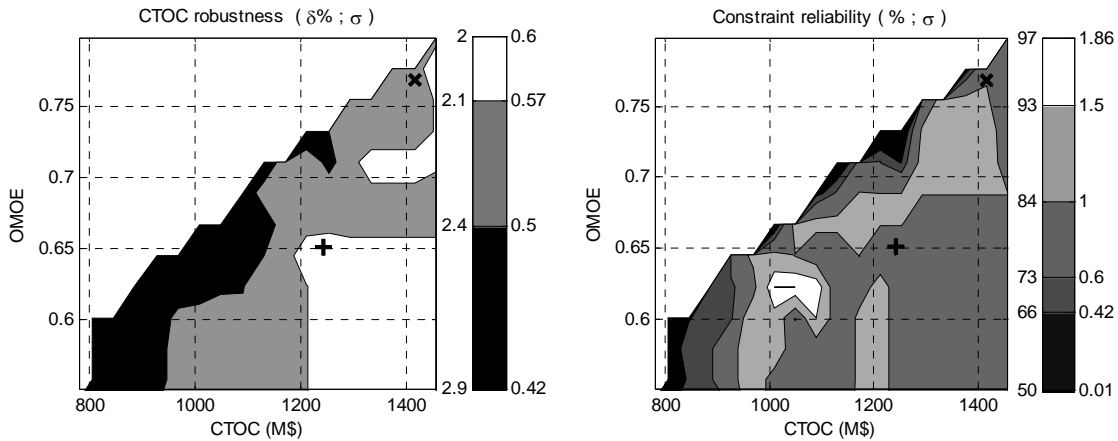
Figure 28.1, *left   Pareto optimal set CTOC coefficient of variance.*
***Figure 28.2**, right   Worst case constraint reliability.*

Due to the severe impact of the reduced CTOC limit, CTOC variance is expected to be the weakest link in the quest for high CoS solutions. This expectation is confirmed by comparing the probability levels of Figures 28.1 and 28.2. Figure 29.1 merges these figures and displays the least favorable probability of any CoS criteria in the objective space (considering constraints and CTOC deviation). The CTOC criterion is prevailing throughout the objective space (note the similarity to Figure 28.1), except in some regions close to the 0% CoS Pareto front.

In Figure 29.1, the region around (1400, 0.72) still looks promising for finding high CoS solutions. However, since the sensitivity analysis does not reflect criteria correlation, that region actually does not yield the highest CoS values. As seen earlier, in Figures 15.1 and 15.4, the VS constraint error value function has its gradient almost orthogonal to CTOC, and thus reduces CoS. Also, some constraints are implemented on the opposite side of the RV mean values from the CTOC LSF (see Figure 18). Thus while each criteria may exclude a small portion of the random variable space, those portions may not overlap.

This means that even though a solution shows robustness or reliability, there is no guarantee that the solution has a favorable CoS. To determine an accurate CoS for an individual solution, correlation has to be part of the equation. Even though the reliability is above 72% around (1400, 0.72) in Figure 29.1, the confidence of success in this region, as seen in Figure 29.2, is predicted to be only about 60%. The criteria correlation influence on CoS is apparent.

Figure 29.1, *left   Worst case probability of feasibility of the optimal solutions.*
Figure 29.2, *right   Contour plot of the Pareto front in Figure 26.*

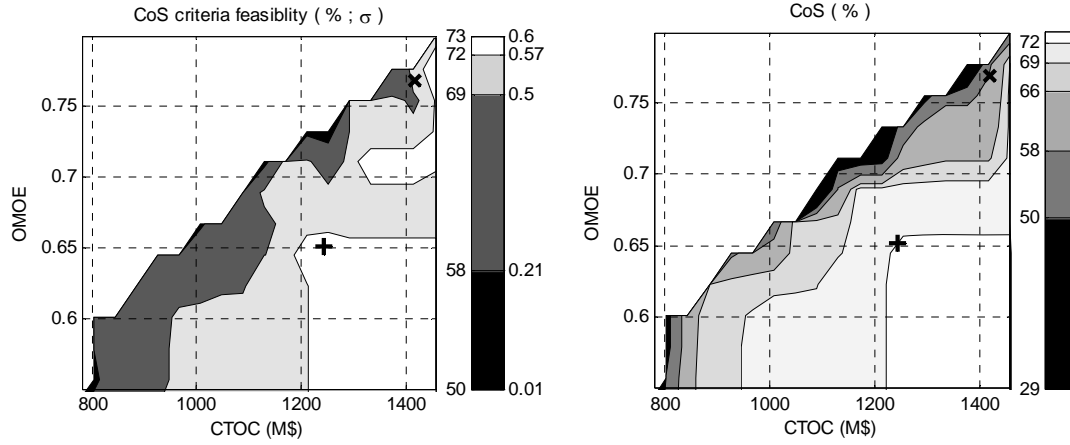The solutions plotted in the last couple of figures are not obtained in an optimization for reliability nor robustness in the common sense. Hence, the comparison with CoS is not completely fair and is purely done to emphasize the effect of criteria correlation.

6   Discussion

The introduction of the term CoS is not done in order to undermine or taint the term probability of success (POS), established by D. N. Mavris et al. CoS is more or less a layman appealing namesake of POS, explicitly intended as an unbiased objective in the optimization process.

Implementation of MV in the CoS calculation in the demonstration is done quite roughly, and it would most certainly be possible to reduce both the errors and computational time without too much effort. However, the general problem with approximation of non-linear functions will remain. A first order Taylor series expansion, i.e. MV, isn't enough to approximate a not-so-well-behaved response, e.g. OMOE. Furthermore, MV will not reveal that there might be a problem with the approximation of this response. One extra system evaluation at the MPP may identify approximation problems. One extra evaluation should be enough to reveal functions such as OMOE in the demonstration as critical for a first order approximation. This extra evaluation could also be used to improve the LSF approximations of all criteria. Adjusting MV with extra evaluations is a step closer to AMV, but the necessity of a complete CDF correction is questionable because of the increased computational burden, and highly non-linear or discontinuous functions will not be approximated accurately anyway. Since the Taylor series expansion can also be used for sensitivity measures, additional metrics such as criteria variance can be incorporated in the optimization process. This would allow implementation of, for example, low variance objectives or constraints.

Separating objectives and constraints in the CoS calculation for reliability and robustness respectively may be an interesting (and more traditional) approach. This would mean adding more objectives and/or constraints, which would ultimately prolong the optimization. Also, if the objective space is expanded beyond three dimensions, it may be more difficult for the decision maker to interpret the optimization results.

6.1 Demonstration

CoS is defined as the probability that a design solution will perform as predicted. The calculated CoS value for the Arleigh Burke class design in the simplified model used in the demonstration is just below 0.6, which suggests that there is a 40% risk that this design would not live up to expectations. However, calculations and assumptions in this work are only an academic exercise to demonstrate the capability and usability of CoS and MV. To be able to do a CoS calculation in closer agreement with reality, there is a need to accurately represent all sources of uncertainty.

Even though the approach to calculate CoS in this paper looks promising for well-behaved responses, further exploration has to be done. Only two normally distributed random variables have been used within the system, and the probabilistic characteristics

of those are only assumed; they have no statistical background. The actual characteristics of the uncertain variables have to be explored before implementation.

The incorporation of more variables will call for a greater number of iterations to numerically derive the approximate response functions and thus increase the total computational burden (See Table 7). Also, the effect of additional variables on criteria responses has to be explored. If additional variables are shown to have significant nonlinear effects on responses, other approximation methods might have to be considered. If the number of uncertain variables becomes extremely large, maybe even the use of Descriptive Sampling[1,7] will pay off, since this method, like MCS, is insensitive to the number of variables.

7   CONCLUSION

By including CoS in the optimization process, decision makers will have a better chance of choosing and/or further evolving a both robust and reliable concept or design, i.e. decide on a design with satisfactory assurance of performing as predicted.

The demonstration emphasizes the importance of looking at the correlation of all design criteria concurrently. For example, commonly formulated robust or reliability optimization, where low criteria variance almost becomes an aim in its own, does not reflect the actual CoS of a design solution since correlation is not considered. A reliability formulation may be sufficient if it is possible (and desirable) to find solutions with extremely high reliability for each individual criteria concurrently. However, such solutions ought to be more interesting (and desirable) for mass production designs than for large one-off or short series products, e.g. navy vessels.

Calculation of CoS via MV, i.e. first order Taylor series expansion, does not guarantee that the objective space has been accurately explored in the optimization process, unless all CoS criteria functions are known to be well-behaved throughout the objective space. For this reason, a first order approximation of criteria responses in unknown objective space should only be used as guidance in preliminary or conceptual design situations. However, one or a few extra system evaluations at each DP may be enough to reveal high risk of poor accuracy in the approximation and thus allow special treatment of those individuals.

For systems with few uncertainties, MV is quite efficient. In the demonstration, with two embedded uncertainties, CoS is calculated with only 3 system evaluations and it closely approximates a MCS of several thousand system evaluations.

8   <u>ACKNOWLEDGMENTS</u>

9   REFERENCES

1   Koch, P. N., Cofer, J. I.; *Simulation-based design in the face of uncertainty,* JANNAF Interagency Propulsion Committee, 2nd Modeling and Simulation Subcommittee, Destin, FL, Apr. 8-12, 2002.

2   Mavris, D. N., Bandte, O., DeLaurentis, D. A.; *Determination of system feasibility and viability employing a joint probabilistic formulation*, AIAA-1999-0183, Aerospace Sciences Meeting and Exhibit, 37th, Reno, NV, Jan. 11-14, 1999.

3   Du, X., Chen, W.; *Efficient uncertainty analysis methods for multidisciplinary robust design,* AIAA Journal, 0001-1452, vol. 40, no. 3, pp. 545-552, 2002.

4   Parsons, M. G., Scott, R. L.; *Formulation of multicriterion design optimization problems for solution with scalar numerical optimization methods,* Journal of Ship Research, vol. 48, no. 1, pp. 61-76, 2004.

5   Haldar, A., Mahadevan, S.; *Probability, reliability and statistical methods in engineering design*, ISBN0471331198, John Wiley & Sons, New York, 2000.

6   Handscomb, D.C., Hammersley, J.M.; *Monte Carlo methods*, ISBN0412158701, Chapman and Hall, London, 1964.

7   Saliby, E., *Descriptive Sampling: An improvement over Latin Hypercube Sampling*, Proceedings of the 29th Winter Simulation Conference, Atlanta, GA, Dec. 7-10, 1997, pp. 230-233, ISBN078034278X, ACM Press, New York, 1997.

8   Avramidis, A. N., *Variance reduction for quantile estimation via correlation induction*, Proceedings of the 1992 Winter Simulation Conference, Arlington, VA, Dec. 13-16, 1992.

9   Kamal, H. A., Ayyub, B. M., *Variance reduction techniques for simulation-based structural reliability assessment of systems*, PMC2000-155, 8th ASCE Specialty Conference on Probabilistic Mechanics and Structural Reliability, Notre Dame, IN, Jul. 24-26, 2000.

10   Thacker, B. H., Nicolella, D. P., Kumaresan, S., Yoganandan, N., Pintar, F. A.; *Probabilistic Finite Element Analysis of the human lower cervical spine,* Journal of Mathematical Modeling and Scientific Computing 13, no. 1-2, pp. 12-21, 2001.

11   Mavris, D. N., Mantis, G. C., Kirby, M. R.; *Demonstration of a probabilistic technique for the determination of aircraft economic viability*, AIAA-1997-5585, AIAA and SAE World Aviation Congress, Anaheim, CA, Oct. 13-16, 1997.

12   Riha, D. S., Thacker, B. H., Millwater, H. R., Wu, Y.-T.; Enright, M. P.; *Probabilistic engineering analysis using the NESSUS software*, AIAA-2000-1512, AIAA/ASME/ASCE/AHS/ASC Structures, Structural Dynamics, and Materials Conference and Exhibit, 41st, Atlanta, GA, Apr. 3-6, 2000.

13   *NESSUS Theoretical manual Version 7.0*, Southwest Research Institute, 2001.

14   Blom, G.; *Probability and statistics: theory and applications*, ISBN0387968520, Springer Verlag, New York, 1989.

15   Brown, A., Thomas, M.; *Reengineering the naval ship concept design process,* ASNE/SNAME From Research to Reality in Ship Systems Engineering Symposium, Tysons Corner, VA, Sep. 18-19, 1998.

16   Hwang, C.-L., Yoon, K.; *Lecture notes in economics and mathematical systems, vol. 186; Multiple attribute decision-making: Methods and applications*, ISBN0387105581, Springer Verlag, New York, 1981.

APPENDIX 1: Model input parameters, DDG51 DP and design variable boundaries.

Parameter		DDG51	min	max	parameter	type
Emin	Endurance range threshold (NM)	3500			fixed	constraint
GMmax	Max GM to beam ratio	0.15			fixed	constraint
GMmin	Min GM to beam ratio	0.05			fixed	constraint
Vsmin	Min sustained speed (knots)	28			fixed	constraint
B	Waterline beam (m)	18	9	27	continuous	variable
Cp	Prismatic coefficient	0.615	0.51	0.72	continuous	variable
Cx	Section coefficient	0.822	0.72	0.93	continuous	variable
D10	Hull depth at station 10 (m)	12.7	6	19	continuous	variable
Lwl	Waterline length (m)	142	118	166	continuous	variable
T	Draft (m)	6.1	3	10	continuous	variable
TS	Stores duration (days)	60	60	90	continuous	variable
VD	Deckhouse volume (m^3)	5437	1000	6500	continuous	variable
Ve	Endurance speed (knots)	20	20	40	continuous	variable
AAW	Anti-Air Warfare system	2	1	4	discrete	variable
ASuW	Anti-Surface Warfare system	2	1	2	discrete	variable
ASW	Anti-Submarine Warfare system	1	1	5	discrete	variable
BALtyp	Ballast type	1	0	1	discrete	variable
C4I	C4 and intelligence system	1	1	2	discrete	variable
CDHmat	Deckhouse material type	1	1	2	discrete	variable
Gsys	Generator system	3	1	4	discrete	variable
MCM	Mine Counter Measures	3	1	3	discrete	variable
NCPS	Collective protection system	2	0	2	discrete	variable
Nfins	Pair of fins	0	0	1	discrete	variable
NSFS	Naval Surface Fire Support system	2	1	3	discrete	variable
Psys	Propulsion system	6	1	15	discrete	variable
SEW	Space and Electronic Warfare system	1	1	3	discrete	variable
STK	Strike warfare system	2	1	2	discrete	variable
VLS	Vertical Launching System	2	1	4	discrete	variable
Ca	Correlation allowance	0.0004			fixed	parameter
Cman	Manning factor	1			fixed	parameter
CRD	Raised deck coefficient	0.8			fixed	parameter
E24mf	Electrical 24 hour design load margin	1.05			fixed	parameter
EDmf	Electrical design and growth margin	1.05			fixed	parameter
EFmf	Electrical fault margin factor	1.05			fixed	parameter
flare	Hull flare angle (degrees)	10			fixed	parameter
FP	Profit margin	0.1			fixed	parameter
HDK	Mean deck height	2.9			fixed	parameter
KGmarg	Center of gravity margin factor	0.25			fixed	parameter
LS	Service life (years)	30			fixed	parameter
Pmf	Propulsion margin factor	1.08			fixed	parameter
RD	Discount rate	0.1			fixed	parameter
RI	Average lead ship inflation rate	10			fixed	parameter
RIF	Average follow ship inflation rate	5			fixed	parameter
RP	Production rate (per year)	2.5			fixed	parameter
Wmf	Weight margin factor	0.005			fixed	parameter
NS	Number of ships	20			fixed	parameter
NYbase	Base year	1985			fixed	parameter

APPENDIX 2: OMOE weight factor vector.

All performance attributes produce a Measure Of Performance (MOP) value between 0 and 1. The dot product of the MOP and weight factor vector generate the OMOE value, ranging between 0 and 1. The weight factors are attuned to the mission/ship type at hand, based on expert opinion.

MOP weight factor	Performance attribute
0.090	Anti-Air Warfare system
0.088	Anti-Surface Warfare system
0.065	Anti-Submarine Warfare system
0.084	Mine Counter Measures
0.048	Naval Surface Fire Support system
0.097	C4 and intelligence system
0.055	Space and Electronic Warfare system
0.034	Strike warfare system
0.082	Vertical Launching System
0.052	Endurance Range
0.032	Stores Duration
0.019	Sustained Speed
0.049	Seakeeping
0.032	Number of shafts
0.043	Structural Vulnerability
0.032	Number of shafts
0.014	Collective protection system
0.012	IR Signature
0.014	Acoustic Signature
0.018	Topside Radar Cross Section
0.037	Magnetic Signature / Degaussing
1.000	

APPENDIX 3: Numerical differentiation, Visual Basic script.

Sets up the CoS (numerical differentiation) GUI in ModelCenter and produce the necessary criteria responses for CoS calculation.

```
distVariable.autoGrow = true
distResponse.autoGrow = true
createRefProps()

sub run
        numVar = distVariable.length              'number of uncertain variables
        numResp = distResponse.length             'number of criteria
        Z.setDimensions numVar+1,numResp          'criteria response matrix
        X.setDimensions numVar+1,numVar           'RV input matrix
        Zls.setDimensions numResp                 'limit state values
        UL.setDimensions numResp                  'specify infeasible regions

        iter = 0
        break = 0

        do until iter > numVar                    'generate Z and X via distVar (i.e. Δ-step)

                if iter = 0 then
                        distVariable(numVar - 1) = 0
                end if

                if iter > 0 then
                        distVariable(iter - 1) = distVariable.getRefPropValue("step",iter-1)
                end if

                if iter > 1 then
                        distVariable(iter - 2) = 0
                end if

                for i = 0 to numResp - 1
                        Z(iter,i) = distResponse(i)

                        if iter = 0 then
                                UL(i) = distResponse.getRefPropValue("overUnder",i)
                                limit = distResponse.getRefPropValue("limitState",i)

                                if limit = 0 then
                                        Zls(i) = 0
                                else
                                        Zls(i) = distResponse(i)*(1+limit)
                                end if
```

54

```
                    if i > 1 then
                            if distResponse(i) < 0 then
                                    break = numVar
                            end if
                    end if
              end if
        next

        iter = iter + 1 + break
        totIter = totIter + 1
    loop

    for i = 0 to numVar - 1
          X(i+1,i) = distVariable.getRefPropValue("step",i)
    next
end sub

sub createRefProps()         'creates the appropriate reference properties in the GUI
    dim prop
    set prop = distVariable.createRefProp( "step", "double" )
    prop.title = "Step"
    prop.description = "step size of N(0,1)"
    set prop = distResponse.createRefProp( "limitState", "double" )
    prop.title = "Limit state ratio from mean"
    prop.description = "limit sate"
    set prop = distResponse.createRefProp( "overUnder", "double" )
    prop.title = "Over (1) / under (0) not wanted"
    prop.description = "Values over (1) / under (0) not wanted"
end sub
```

APPENDIX 4: Probability calculation, Matlab.

Calculates CoS and each individual criterions probability of feasibility.

```
respnum = length(Z(1,:));                    %number of responses of interest
varnum = length(Z(:,1)) - 1;                 %number of standard normal distributed variables
X = [ones(max(size(X)),1) X];                %variable expansion values
span = 5;                                     %+/- limiting of (standard normal) distributed variables
respjpdf = [];
meanZ = Z(1,:)';                             %mean/deterministic value of each criteria
if any(Z(1,3:respnum)<0)                      %catch infeasible mean value
      CoS = 0;
      respPoF = zeros(respnum,1);
      Z(2:varnum+1,:) = 0;
      A = zeros(varnum+1,respnum);
else
      for i = 1:respnum
            A(:,i) = X \ Z(:,i);             %produces A vector for every criteria
      end
      t = logspace(0,log(span+1)/log(10),ceil(span*25))-1;
      tint = [t 0]-[0 t];
      t = [0 t] + tint/2;
      t = t(2:length(t)-1);
      tint = tint(2:length(tint)-1);
      ttemp = [-rot90(t); t'];
      for i = 1:respnum
            [Yz,Xz,LS] = ndgrid(A(3,i)*ttemp,A(2,i)*ttemp,A(1,i)-Zls(i));
            check = Xz + Yz + LS;     %create limit state values for all coordinates
            if UL(i) = = 1                    %UL: 1 - removal of values > Zls , 0 - removal of values < Zls
                  area = (check + abs(check));      %OBS, creates zeros
            else
                  area = (check - abs(check));      %OBS, creates zeros
            end
            respjpdf(:,:,i) = isnan(area ./ area);      %creates ones in place of NaN
      end
      domain = prod(respjpdf,3);
      jpdf = (normpdf(t)' * normpdf(t)) .* (tint' * tint);
      jpdf = [fliplr(jpdf) jpdf];
      jpdf = [flipud(jpdf); jpdf];
      CoS = sum(sum(domain .* jpdf));         %Calculate the CoS value
      respPoF = squeeze(sum(sum(respjpdf .* repmat(jpdf,[1 1 respnum]))));   %Probability of feasibility
                                                                            %for each criterion
end
```

APPENDIX 5: DDG51 and Pareto optimal solutions.

The table shows the characteristics of some of the design solutions of the Pareto optimal set from the optimization run presented in section 5.2 Optimization, implementing Confidence of Success.

Solution	DDG51 DP	CTOC DP	OMOE DP	CoS DP	Best DP	DP1	DP2

Objective

	DDG51 DP	CTOC DP	OMOE DP	CoS DP	Best DP	DP1	DP2
CoS	0.58	0.40	0.38	0.97	0.86	0.71	0.73
CTOC(M$)	1417.6	741.9	1394.1	1285.4	967.0	1267.3	1374.5
OMOE	0.77	0.55	0.83	0.65	0.66	0.79	0.82

Constraint error value

	DDG51 DP	CTOC DP	OMOE DP	CoS DP	Best DP	DP1	DP2
TA	0.09	0.29	0.19	0.21	0.10	0.13	0.16
DA	0.31	0.06	0.05	0.87	1.06	0.06	0.04
VS	0.15	0.01	0.01	0.07	0.14	0.11	0.09
KW	0.16	0.97	0.20	0.44	0.67	0.37	0.06
GMmin	0.68	0.92	0.62	0.85	1.06	1.41	0.72
GMmax	0.44	0.36	0.46	0.38	0.31	0.20	0.43
D10	0.11	0.02	0.13	0.19	0.03	0.09	0.13
E	0.25	0.06	0.06	0.75	1.45	0.69	0.58

Individual CoS criterion feasibility probability

	DDG51 DP	CTOC DP	OMOE DP	CoS DP	Best DP	DP1	DP2
CTOC	0.98	0.97	0.97	0.98	0.98	0.98	0.97
OMOE	1.00	1.00	1.00	1.00	0.91	1.00	1.00
TA	0.96	1.00	1.00	1.00	0.96	0.98	0.99
DA	1.00	1.00	1.00	1.00	1.00	1.00	1.00
VS	1.00	0.75	0.72	1.00	1.00	1.00	1.00
KW	1.00	1.00	1.00	1.00	1.00	1.00	1.00
GMmin	0.97	0.99	0.90	0.99	1.00	1.00	0.93
GMmax	1.00	1.00	1.00	1.00	1.00	0.93	1.00
D10	1.00	1.00	1.00	1.00	1.00	1.00	1.00
E	0.62	0.52	0.52	0.98	0.97	0.78	0.73

Embedded attribute

	DDG51 DP	CTOC DP	OMOE DP	CoS DP	Best DP	DP1	DP2
RT (kN)	100889	71944	108885	304106	94410	101610	109821
WT (t)	7905	6001	10878	7914	6836	9061	10094

Solution	DDG51 DP	CTOC DP	OMOE DP	CoS DP	Best DP	DP1	DP2

Design variable

B (m)	18.0	16.1	20.7	18.6	17.7	20.1	20.6
Cp	0.615	0.51	0.51	0.60	0.51	0.51	0.51
Cx	0.822	0.72	0.72	0.80	0.80	0.72	0.72
D10 (m)	12.7	12.6	16.6	15.8	13.4	15.4	16.7
Lwl (m)	142.0	146.2	155.9	140.0	147.7	151.7	155.8
T (m)	6.1	6.8	8.7	8.0	7.4	8.3	8.7
TS (days)	60	68	86	82	69	80	69
VD (m^3)	5437	1100	4000	2400	2400	2600	4000
Ve (knots)	20.0	20.0	20.1	27.7	20.7	20.0	20.2
AAW	2	4	2	4	4	4	2
ASuW	2	1	1	1	1	1	1
ASW	1	5	2	4	5	1	2
BALtype	1	1	0	1	1	0	0
C4I	1	1	1	1	1	1	1
CDHmat	1	2	2	1	1	1	1
Gsys	3	3	3	3	3	3	3
MCM	3	2	1	2	1	1	1
NCPS	2	0	1	0	0	2	1
Nfins	0	0	0	0	0	0	1
NSFS	2	1	1	2	1	1	1
Psys	6	2	12	6	6	6	6
SEW	1	1	1	1	1	1	1
STK	2	2	1	2	2	2	1
VLS	2	4	3	4	4	3	4